[American Journal of Science, Vol. 315, March, 2015, P. 167–203, DOI 10.2475/03.2015.01]

American Journal of Science

MARCH 2015

CATABOLIC RATES, POPULATION SIZES AND DOUBLING/REPLACEMENT TIMES OF MICROORGANISMS IN NATURAL SETTINGS

DOUGLAS E. LaROWE*,† and JAN P. AMEND*,**

ABSTRACT. Directly assessing the impact of subsurface microbial activity on global element cycles is complicated by the inaccessibility of most deep biospheres and the difficulty of growing representative cultivars in the laboratory. In order to constrain the rates of biogeochemical processes in such settings, a quantitative relationship between rates of microbial catalysis, energy supply and demand and population size has been developed that complements the limited biogeochemical data describing subsurface environments. Within this formulation, rates of biomass change are determined as a function of the proportion of catabolic power that is converted into anabolism—either new microorganisms or the replacement of existing cell components—and the amount of energy that is required to synthesize biomass. Catabolic power is related to biomass through an energy-based yield coefficient that takes into account the constraints that different environments impose on biomolecule synthesis; this method is compared to other approaches for determining yield coefficients. Furthermore, so-called microbial maintenance energies that have been reported in the literature, which span many orders of magnitude, are reviewed. The equations developed in this study are used to demonstrate the interrelatedness of catabolic reaction rates, Gibbs energy of reaction, maintenance energy, biomass yield coefficients, microbial population sizes and doubling/replacement times. The number of microorganisms that can be supported by particular combinations of energy supply and demand is illustrated as a function of the catabolic rates in marine environments. Replacement/doubling times for various population sizes are shown as well. Finally, cell count and geochemical data describing two marine sedimentary environments in the South Pacific Gyre and the Peru Margin are used to constrain *in situ* metabolic and catabolic rates. The formulations developed in this study can be used to better define the limits and extent of life because they are valid for any metabolism under any set of conditions.

Keywords: bioenergetics, maintenance energy, power, biomass yield coefficients, reaction rates, catabolism, doubling/replacement time, thermodynamics

INTRODUCTION

Microorganisms have significantly modified the Earth's atmosphere, hydrosphere and lithosphere throughout most of geologic history. Through their metabolic activities they have contributed significantly to the oxygenation of Earth's atmosphere, altered mineral weathering rates and influenced global element cycling. These transformations are a byproduct of the microbial demand for energy associated with maintaining basic cellular functions, biomass synthesis and growth. In order to better understand the connections between the microbiological demand for energy and the

* Department of Earth Sciences, University of Southern California, Los Angeles, California 90089-0740, USA

** Department of Biological Sciences, University of Southern California, Los Angeles, California 90089-0371, USA

† Corresponding author: Email: larowe@usc.edu; Phone: (213) 821-2268

impact that this has on their environment, numerous field and laboratory studies have been carried out examining the metabolisms of microorganisms that live in near-surface environments such as phototrophs, aerobic heterotrophs and microorganisms that affect human activities. As a result, much has been learned about the growth rates, nutrient requirements and molecular functioning of organisms in these high-energy environments.

Over the past three decades, however, it is has become clear that microorganisms inhabit a far greater diversity of environments than previously appreciated, such as hydrothermal systems, deep marine and freshwater sediment, hydrocarbon reservoirs, unconsolidated sedimentary rock, shale, sandstone, fractured granite, deep aquifers, caves, mines, paleosols, aquitards, permafrost and more (Amy and Haldeman, 1997; Fredickson and Fletcher, 2001; Steven and others, 2006; Orcutt and others, 2011; Strapoć and others, 2011; Edwards and others, 2012). Many of these environments can be described as low-energy systems that host poorly characterized organisms growing at rates far slower than what was thought possible (Roszak and Colwell, 1987; Lennon and Jones, 2011). In particular, the observation of intact microbial cells in cores from marine deep sediments have led to new estimates of the Earth's biomass carbon (for example, Whitman and others, 1998; Kallmeyer and others, 2012). Demonstrations of their viability (Morono and others, 2011) and calculated doubling/replacement times of thousands of years (Jørgensen, 2012) have raised fundamental questions about the activity levels, extent, evolution, survival and limits of life. As a result, laboratory-determined values for basic aspects of microbial physiology such as catabolic rates, maintenance energy and biomass yield are being called into question (Hoehler and Jørgensen, 2013). In effect, the conditions under which microorganism are grown in the laboratory are so different from those that organisms encounter in the extreme biosphere that it is unclear how laboratory-measured and derived physiological properties apply to these natural settings. Here, we describe a quantitative approach for characterizing the physiology of microorganisms in any environment, but with special emphasis on the subsurface. After a discussion of the nature and extent of the deep biosphere, this model is described.

THE DEEP BIOSPHERE

Due to its potential size (Whitman and others, 1998; Kallmeyer and others, 2012) and long-term effect on global geochemical cycles, the focus of this study is directed towards microbial habitats that are located in marine sediments at or below the sediment water interface, SWI. Some or all of these environments could fall within the designation 'deep biosphere', although this is an ambiguous term characterized by conflicting descriptions. The reason that there is no clean-cut definition for where the deep biosphere begins is because the guidelines that have been suggested for delineating the boundaries of deep ecosystems are motivated by parochial interests. For instance, scientists studying marine sedimentary environments typically define the deep biosphere as being a certain number of meters beneath the sediment water interface (Fredickson and others, 1989; Whitman and others, 1998; Jørgensen and Boetius, 2007; Edwards and others, 2012; Hoehler and Jørgensen, 2013). This definition cannot be applied to terrestrial settings or even many marine habitats that are not covered by sediments, but that nonetheless could be considered the deep biosphere: seamounts, new oceanic crust and some hydrothermal systems (Jørgensen and Boetius, 2007; Orcutt and others, 2013). Similarly, many of the definitions for terrestrial deep habitats would exclude marine sediments as comprising part of the deep biosphere. For example, Fredickson and Onstott (2001) suggest that the deep biosphere be limited to environments in which microorganisms must rely upon endogenous sources of energy. Similarly, Stevens (1997) maintains that the deep biosphere cannot be dependent on photosynthetically produced organic matter. Lovley and Chapelle (1995) argue that terrestrial deep ecosystems are those that are not hydrologically

well-connected to the surface world, and go so far as to proscribe that deep systems should be characterized as having groundwater flow < 1 m/yr. Alternatively, Whitman and others (1998) define deep terrestrial habitats as being more than 8 m beneath the surface and McMahon and Parnell (2014) use cell count data from between 10 and 3600 m to estimate the biomass of deep terrestrial environments. Edwards and others (2012) simply state that deep ecosystems are 1 m or more below the continental surface and SWI. Other environments that might be classified as deep habitats such as caves, mines, hydrocarbon reservoirs, permafrost or the space in and under glaciers and ice sheets do not meet at least one of the above listed criteria for what makes a deep biosphere, yet many are considered as such.

Because the model developed in this communication is applied to marine sediments, it is worth noting what the term "deep biosphere" means with respect to sediments and how this definition has changed. Fredickson and others (1989) stipulate that it starts 10 m under the SWI, while D'Hondt and others (2009) note that earlier studies consider 1.5 m below the SWI to be a boundary line. Jørgensen and Boetius (2007) state in their review that the deep-sea bed is > 1 m beneath the SWI, a depth that they note as typically being beneath the depth of oxygen penetration and the extent of burrowing animals. Whitman and others (1998) define deep marine sediments as being 10 cm beneath the SWI. In many of the studies that discuss the size of the deep biosphere, cell count data less than one cm below the SWI are considered (for example, Parkes and others, 1994; Parkes and others, 2000; D'Hondt and others, 2004; D'Hondt and others, 2009; Kallmeyer and others, 2012). In fact, Kallmeyer and others (2012) only used data from cores that had cell counts above and below 1 m beneath the SWI in their estimate of global biomass in marine sediments. Hoehler and Jørgensen (2013) somewhat vaguely define the deep biosphere as "the set of ecosystems and their organisms living beneath the upper few meters of the solid earth surface." Some reviews on the deep biosphere simply refer to a dark biosphere rather than a deep one (Orcutt and others, 2011; Edwards and others, 2012) to indicate that it is the absence of photosynthesis that distinguishes them, similar to some of the definitions used for the terrestrial deep biosphere (Stevens 1997; Fredickson and Onstott, 2001). Other reviews on the topic of the deep biosphere avoid defining the term altogether (Guerrero, 1998; Teske, 2005; Colwell and D'Hondt, 2013). Due to the numerous environments in which microorganisms have been found and the variety of variables that can be used to define their habitats, perhaps it is a fool's errand to issue a globally relevant definition of the deep biosphere. In the end, such a definition is not required for the purposes of this study since the model presented is applicable for quantifying microbial activity in any environment.

Marine sediments are an ideal setting for demonstrating how energy availability determines the level of microbial activity and amount of biomass in an environment due to the rich variability and size of sedimentary environments. They can vary by the prevailing types and sizes of mineral grains, porosity, temperature gradients, amount and quality of organic matter, pore water composition, the degree to which the SWI zone is bioturbated and/or bioirrigated, their thickness, how much water overlies them, their distance from land, whether they sit on continental or oceanic crust, contain variable amounts of clathrates, span many millions of years in age and can harbor organisms from all three domains of life. With such physical, compositional and biological diversity, it is no wonder that the number of microbial cells found in a cubic centimeter of marine sediments can vary by many orders of magnitude (Kallmeyer and others, 2012). In addition to their heterogeneity, marine sediments cover $\sim$70 percent of Earth's surface, contain something on the order of 10^{29} to 10^{30} prokaryotic cells (Whitman and others, 1998; Kallmeyer and others, 2012) and host at least the early stages of petroleum formation. It should be noted that these biomass estimates do

not take into account the vast habitable pore space in the oceanic lithosphere (Orcutt and others, 2011), where it has been estimated that 10^{12} g of cellular carbon are produced each year exclusively from the energy gained by catalyzing water-rock interactions (Edwards and others, 2012).

Despite the extremes in temperature, pressure, pH and other compositional factors that microorganisms in marine sediment and many other environments face, most share the ability to live under very low energy conditions (Jørgensen and Boetius, 2007; Jørgensen, 2011; Jørgensen, 2012). One of the consequences of living in such low energy systems is long turnover times compared to their surface-dwelling analogs (Thorn and Ventullo, 1988; Parkes and others, 1990; Konopka, 2000; D'Hondt and others, 2002). For example, bacteria in aquifers (Phelps and others, 1994), sedimentary rocks (Chapelle and Lovley, 1990; Phelps and others, 1994), marine (D'Hondt and others, 2004; Schippers and others, 2005; Jørgensen and D'Hondt, 2006; Lomstein and others, 2012; Røy and others, 2012) and freshwater sediments (Thorn and Ventullo, 1988) and ice cores (Price and Sowers, 2004) appear to have turnover times exceeding 1000 years. Even photosynthetic microbial communities in Antarctica appear to have biomass turnover times of up to 19,000 years (Johnston and Vestal, 1991). Taken together, a significant proportion of the world's microorganisms seem to be adapted to not only low-energy fluxes, but extremely low metabolic activity. Although the relationships between energy supply, energy demand, and the rates of microbially catalyzed processes for most subsurface organisms are unclear (Jørgensen, 2011), relating these variables in a coherent mathematical expression can reveal quantitative connections among them.

QUANTIFYING BIOMASS CHANGE

Catabolic rates, maintenance energy and biomass yield can be combined with a thermodynamic description of anabolism (biomass synthesis) and catabolism (ATP generation) to generate an equation that relates all of these bioenergetic parameters to microbial growth rates and population sizes in the deep biosphere. The approach taken to accomplish this compares the rate of energy realized through catabolism to the rate at which catabolic energy is dissipated through a collection of activities, including what is generally called maintenance energy (Pirt, 1965; Russell and Cook, 1995; van Bodegom, 2007). Biomass yield—either new cells or simply the replacement of existing cellular components—is computed from the energy of biomolecular synthesis, which is dependent on environmental conditions.

Power (P), which couples the energy available in a system with the rate at which it is processed or dissipated, constrains the potential for biomass synthesis in a given environment. As a result, the most appropriate unit for describing the dynamics of microbial biomass changes is the Watt (see Shock and Holland, 2007). Therefore, the formulations developed below are related to one another through power.

Power Supply

The amount of power available to microorganisms, the power supply—P_s, from a given catabolic reaction is simply the Gibbs energy, ΔG_r, of that reaction multiplied by its rate, r. This is represented symbolically by

$$P_s = \left|\frac{\Delta G_{r,j}}{\nu_i}\right| \cdot r_j \tag{1}$$

where j refers to the reaction of interest and ν_i, represents the stoichiometric coefficient of a particular reactant or product in the jth reaction. Values of ν_i are required to evaluate equation (1) in order to ensure that the calculated values of ΔG_r are consistent with the units for the reaction rates: for some catabolic reactions, rates

TABLE 1

Glossary of symbols

Symbol	Definition	Units
a_i	activity of the *i*th sepcies	-
B_j	biomass resulting from the *j*th reaction	cell, cell cm^{-3}
$B_{j,0}$	biomass resulting from the *j*th reaction at $t = 0$	cell, cell cm^{-3}
$B_{j,t}$	biomass resulting from the *j*th reaction at *t*	cell, cell cm^{-3}
D	biomass decay constant	t^{-1}
ΔG_r	Gibbs energy of reaction	J mol^{-1}
ΔG_r^0	Standard state Gibbs energy of reaction	J mol^{-1}
K_j	equilibrium constant of the *j*th reaction	-
P_{cs}	cell-specific maintenance power requirement	W $cell^{-1}$
P_d	dissipated power	W cm^{-3} , W cm^{-2}
P_s	catabolic power supply	W cm^{-3} , W cm^{-2}
Q_j	reaction quotient of the *j*th reaction	-
R	gas constant	J mol^{-1} K^{-1}
r_j	rate of the *j*th reaction	mol cm^{-3} t^{-1}, mol cm^{-2} t^{-1}
T	temperature	°C, K
t	time	s, d, y
$t_{d/r}$	doubling/replacement time	s, d, y
Y_j	Biomass yield resulting from the *j*th reaction	cell J^{-1}
γ_i	activity coefficient of the *i*th species	-
ν_i	stoichiometric coefficient of the *i*th species	-

are reported per mole of reactant (for example, sulfate for sulfate reduction reactions), while in others, a product species fulfills this role (for example, methane for methanogenesis). For ΔG_r in units of J mol^{-1} and r in mol cm^{-3} sec^{-1}, P_s takes on units of *volume-specific* power, W cm^{-3}. A glossary of symbols appearing in this communication is provided in table 1. In order to obtain representative values of P_s, catabolic reaction rates in the marine biosphere were compiled from the literature, and nominal Gibbs energies of the reactions describing these processes were computed.

Catabolic rates.—The rates at which microorganisms catalyze redox reactions can vary by many orders of magnitude. Table 2 provides a selection of measured and modeled catabolic rates in marine environments at and below the SWI located throughout the globe. The catabolic rates vary over twelve orders of magnitude from 6.0×10^{-9} to 6.66×10^{3} nmol cm^{-3} day^{-1} (the reactions are typically reported per mole of a substrate being processed, although sometimes it's given per mole produced). Note that much of this range can be found for a single catabolic reaction and the rates for different reactions overlap. For instance, sulfate reduction rates ($1.0 \times 10^{-6} - 6.66 \times 10^{3}$ nmol cm^{-3} day^{-1}) overlap considerably with those of aerobic methane oxidation ($2 \times 10^{-6} - 5.0 \times 10^{2}$ nmol cm^{-3} day^{-1}) and methanogenesis ($6.0 \times 10^{-9} - 1.24 \times 10^{3}$ nmol cm^{-3} day^{-1}). Similarly, geochemical analyses have been used in reaction rate models to estimate comparably large ranges in the rates of microbial CO_2 production ($10^{-5} - 10^{-15}$ mol CO_2 l^{-1} yr^{-1}) in subsurface aquifers,

TABLE 2

Measured and modeled catabolic reaction rates and corresponding catabolic power, P_s, in a variety of submarine environments

Process or Reaction	Rate, nmol $cm^{-3}d^{-1}$	Environment	Location	Reference	P_s, W cm^{-3}
O_2 reduction	2.7×10^{-6} - 0.027 [a]	Open ocean sediments	North Pacific Gyre	Røy and others (2012)	1.4×10^{-14} - 1.4×10^{-10}
aerobic CH_4 oxidation	1.3×10^{-4} [b]	Marine brine pool	Gulf of Mexico	Wankel and others (2010)	1.2×10^{-12}
aerobic CH_4 oxidation	0.113 [c]	hydrothermal sediments	Manus and Lau Basins	Lein and others (1997)	1.1×10^{-9}
aerobic CH_4 oxidation	0.033- 5.70 [c]	hydrothermal sediments	Guaymas Basin & Juan de Fuca Ridge	Galchenko and others (1989)	3.1×10^{-10} - 5.3×10^{-8}
aerobic CH_4 oxidation	2.0×10^{-6} - 2.89×10^{-2} [c]	hydrothermal plume	Juan de Fuca Ridge	de Angelis and others (1993)	1.9×10^{-14} - 2.7×10^{-10}
aerobic CH_4 oxidation	0 - 3.66×10^{-6} [b]	Marine brine pool	Gulf of Mexico	Wankel and others (2010)	3.4×10^{-14}
AOM	0 - 25 [c]	hydrothermal sediments	Guaymas Basin	Kallmeyer and Boetius (2004)	1.2×10^{-8}
AOM	0.062 - 0.079 [b]	Marine brine pool	Gulf of Mexico	Wankel and others (2010)	3.1×10^{-11} - 3.9×10^{-11}
AOM	0.0022 - 0.024 [a]	Continental margin sediments	Eastern Pacific, near Peru	Biddle and others (2006)	1.1×10^{-12} - 1.2×10^{-11}
AOM	0.3 - 150 [c]	Marine Cold Seep sediments	Gulf of Mexico	Orcutt and others (2005)	1.5×10^{-10} - 7.5×10^{-8}
AOM	0-11 [c]	hypersaline cold seep sediments	Gulf of Cadiz	Maignien and others (2013)	5.5×10^{-9}
AOM	0-10 [c]	Submarine mud volcanoes	Gulf of Cadiz	Niemann and others (2006)	5.0×10^{-9}
CH_4 oxidation	0.042 - 173.62 [c]	Marine sediments	Compilation	Parkes and others (2000)	3.9×10^{-10} - 1.6×10^{-6}
CH_4 oxidation	0.1 - 500 [c]	Marine Cold Seep sediments	Gulf of Mexico	Joye and others (2004)	9.3×10^{-10} - 4.7×10^{-6}
CH_4 oxidation	0 - 220 [c]	Marine Cold Seep sediments	Easten Mediterranean	Omoregie and others (2009)	2.1×10^{-6}
anaerobic OM oxidation	0 - 0.0219 [d]	Shelf and trough sediments	Eastern Pacific, near Peru	Lomstein and others (2012)	2.1×10^{-11}
H_2 oxidation	2740 [b]	Diffuse hydrothermal vent	Juan de Fuca Ridge	Wankel and others (2011)	1.5×10^{-5}
Mn reduction	2.5×10^{-6} - 1.6×10^{-7} [a]	Open ocean sediments	Eastern Equitorial Pacific	Wang and others (2008)	6.9×10^{-15} - 4.4×10^{-16}
sulfate reduction	0-23 [c]	hypersaline cold seep sediments	Gulf of Cadiz	Maignien and others (2013)	2.3×10^{-8}
sulfate reduction	50 - 3200 [c]	Marine Cold Seep sediments	Gulf of Mexico	Orcutt and others (2005)	4.9×10^{-8} - 3.1×10^{-6}
sulfate reduction	0 -5500 [c]	Marine Cold Seep sediments	Gulf of Mexico	Joye and others (2004)	5.4×10^{-6}
sulfate reduction	2 - 70 [c]	mud volcano / seafloor brine	Gulf of Mexico	Joye and others (2009)	2.0×10^{-9} - 6.9×10^{-8}
sulfate reduction	0-25 [c]	Submarine mud volcanoes	Gulf of Cadiz	Niemann and others (2006)	2.5×10^{-8}
sulfate reduction	0 - 4323 [c]	Marine Cold Seep sediments	Easten Mediterranean	Omoregie and others (2009)	4.2×10^{-6}
sulfate reduction	1.8×10^{-6} - 6.8×10^{-5} [a]	Open ocean sediments	Eastern Equitorial Pacific	Wang and others (2008)	1.8×10^{-15} - 6.7×10^{-14}
sulfate reduction	0.05 - 0.107 [b]	Marine brine pool	Gulf of Mexico	Wankel and others (2010)	4.9×10^{-11} - 1.0×10^{-10}
sulfate reduction	13 - 6660 [c]	hydrothermal sediments	Guaymas Basin	Kallmeyer and Boetius (2004)	1.3×10^{-8} - 6.5×10^{-6}
sulfate reduction	1×10^{-6} - 6 [c]	Marine sediments	Continental Margin	Parkes and others (2005)	9.8×10^{-16} - 5.9×10^{-9}
sulfate reduction	2×10^{-4} - 38 [c]	Marine Sediment (bottom)	Aarhus Bay	Holmkvist and others (2011)	2.0×10^{-13} - 3.7×10^{-8}
sulfate reduction	1.1×10^{-3} - 400.3 [c]	Marine sediments	Compilation	Parkes and others (2000)	1.1×10^{-12} - 3.9×10^{-7}

TABLE 2
(continued)

Process or Reaction	Rate, nmol $cm^{-3}d^{-1}$	Environment	Location	Reference	P_s, W cm^{-3}
$H_2 + CO_2 \rightarrow CH_4 + 2H_2O$	0 -27 [c]	Marine Cold Seep sediments	Gulf of Mexico	Orcutt and others (2005)	3.5×10^{-8}
$H_2 + CO_2 \rightarrow CH_4 + 2H_2O$	1.73×10^{-3} - 2.73 [c]	Marine sediments	compilation	Parkes and others (2000)	2.2×10^{-12} - 3.5×10^{-9}
$CH_3COO^- + H_2O \rightarrow CH_4 + HCO_3^-$	1.2×10^{-4} - 60 [c]	Marine Cold Seep sediments	Gulf of Mexico	Orcutt and others (2005)	5.8×10^{-14} - 2.9×10^{-8}
$CH_3COO^- + H_2O \rightarrow CH_4 + HCO_3^-$	74.01 - 1240.2 [c]	Marine sediments	compilation	Parkes and others (2000)	3.6×10^{-8} - 6.0×10^{-7}
methanogenesis	0.015 [c]	Marine sediments	Continental Margin	Parkes and others (2005)	1.9×10^{-11}
methanogenesis	8.96 - 52.3 [c]	Deep ocean sediments	Equatorial Atlantic	Arndt and others (2006)	1.2×10^{-8} - 6.8×10^{-8}
methanogenesis	0 - 0.13 [c]	mud volcano / seafloor brine	Gulf of Mexico	Joye and others (2009)	1.7×10^{-10}
methanogenesis	3.8×10^{-8} - 6.0×10^{-9} [a]	Open ocean sediments	Eastern Equitorial Pacific	Wang and others (2008)	4.9×10^{-17} - 7.8×10^{-18}

[a]modeling; [b]*in situ* mass spectrometry; [c]radioisotope incubation; [d]amino acid racemization data

aquitards, vadose zones, deep rocks and consolidated sediments (Kieft and Phelps, 1997). For a common carbon source (for example, acetate), this range of CO_2 production rates would translate into 1.4×10^{-2} to 1.4×10^{-12} nmol acetate cm^{-3} day^{-1}. Although there is some overlap with the rates for the submarine environments discussed above, the lowest calculated acetate consumption rate in the terrestrial subsurface is more than 2 orders of magnitude lower than the lowest rate given in table 2, methanogenesis as calculated by Wang and others (2008). In order to translate reaction rates into values of power using equation (1), the Gibbs energies of these reactions must be computed.

Reaction energetics.—The amount of energy available from catabolic reactions varies as a function of the temperature, pressure and composition of the system of interest. Within the marine realm, this has been demonstrated in hydrothermal systems (Shock and others, 1995; McCollom and Shock, 1997; McCollom, 2000; Shock and Holland, 2004; McCollom, 2007; LaRowe and others, 2008; Amend and others, 2011; LaRowe and others, 2014), ocean sediments (Schrum and others, 2009; Wang and others, 2010; LaRowe and Amend, 2014; Teske and others, 2014) and basement rock (Bach and Edwards, 2003; Cowen, 2004; Edwards and others, 2005; Boettger and others, 2013). The calculated Gibbs energies of the thermodynamically favored (exergonic) reactions considered in these and other studies vary between approximately 0 and −120 kJ $(mol\ e^-)^{-1}$. In order demonstrate how values of ΔG_r vary by electron acceptor and donor, standard state Gibbs energies, ΔG_r^0, of several half-reactions are listed at temperatures from 0.01 to 150 °C in table 3. The utility of expressing these values as kilojoules per mole of electrons transferred, kJ $(mol\ e^-)^{-1}$, allows for the easy combination of electron donor (ED) and electron acceptor (EA) half reactions, at least in the standard state. For instance, ΔG_r^0 at 25 °C for the aerobic oxidation of H_2 is −131.59 kJ $(mol\ e^-)^{-1}$ (−122.73 + −8.86) while that of Mn^{2+} is only −2.7 kJ $(mol\ e^-)^{-1}$ (−122.73 + 120.03). It is informative to note the range of energy differences between different types of organic EDs. At 25 °C, the difference between aerobic oxidation of oxalate and a type III/IV kerogen is 22.68 kJ $(mol\ e^-)^{-1}$. It can also be seen that values of ΔG_r^0 for these half-reactions can go up (S^0, H_2) or down (NO_3^-, MnO_2) as temperature increases, stay relatively flat (O_2, Mn^{2+}) or display an inflection point (NO_2^-). Furthermore, with the exception of H_2 and oxalate below 50 °C, none of the ED half-reactions have negative ΔG_r^0. This underscores the point that the thermodynamic drive and thus energy for metabolism is dictated by the identity of the electron acceptor, the strength of which varies from −144.35 kJ $(mol\ e^-)^{-1}$ for nitrite reduction to N_2, to −15.04 kJ $(mol\ e^-)^{-1}$ for CO_2 reduction to CH_4. Finally and most critically, once the composition of the system is taken in to account, values of ΔG_r can differ significantly from the values of ΔG_r^0 reported in table 3 (see Appendix and below).

Power in marine settings.—The catabolic reaction rates shown in table 2 can be combined with values of ΔG_r and equation (1) to calculate the amount of volume-specific power available to microorganisms, P_s (W cm^{-3}), in the marine biosphere. The amount of catabolic power realized by microorganisms, per cm^3 sediment or water, spans 12 orders of magnitude (table 2). The power range for methanotrophy (both aerobic and anaerobic), methanogenesis and sulfate reduction are shown graphically in figure 1. As with reaction rates, there is considerable overlap in values of P_s between these different catabolic strategies. The largest power range is seen for methanogenesis, followed closely by sulfate reduction and then aerobic CH_4 oxidation. Even though AOM displays the smallest power range, values of P_s still span nearly 5 orders of magnitude. Of course, the amount of power realized by individual microorganisms depends on the fraction of active cells in each cm^3 of sample. Although cell counts have been done for some of the environments listed in table 2 (de Angelis and others,

TABLE 3

Standard state Gibbs energies, ΔG_r^0 (kJ (mol e^-)$^{-1}$) of selected electron acceptor and donor half reactions as a function of temperature at P = 1 bar

EA/ED	Formula	Half-reaction	0.01°C	25°C	50°C	75°C	100°C	125°C	150°C
EA									
nitrite	NO_2^-	$NO_2^- + 3e^- + 4H^+ \rightarrow 1/2N_2 + 2H_2O$	-143.95	-144.35	-145.01	-145.88	-149.34	-146.65	-143.81
oxygen	O_2	$O_2 + 4e^- + 4H^+ \rightarrow 2H_2O$	-122.50	-122.73	-122.90	-123.05	-123.18	-123.30	-123.40
Mn(IV), pyrolusite	$MnO_{2(cr)}$	$MnO_2 + 4H^+ + 2e^- \rightarrow Mn^{2+} + 2H_2O$	-119.83	-120.03	-120.31	-120.68	-121.12	-121.61	-122.15
nitrate	NO_3^-	$NO_3^- + 5e^- + 6H^+ \rightarrow 1/2N_2 + 3H_2O$	-117.85	-118.31	-118.94	-119.72	-120.63	-121.67	-122.82
Fe(III), magnetite	$Fe_3O_{4(cr)}$	$Fe_3O_4 + 8H^+ + 2e^- \rightarrow 3Fe^{2+} + 4H_2O$	-106.46	-104.15	-101.89	-99.71	-97.59	-95.51	-93.42
Fe(III), ferrihydrite	$FeOOH_{(cr)}$	$FeOOH + 3H^+ + e^- \rightarrow Fe^{2+} + 2H_2O$	-101.53	-100.61	-99.76	-99.00	-98.31	-97.68	-97.06
Fe(III), goethite	$FeOOH_{(cr)}$	$FeOOH + 3H^+ + e^- \rightarrow Fe^{2+} + 2H_2O$	-76.96	-75.92	-74.96	-74.10	-73.31	-72.57	-71.85
Fe(III), hematite	$Fe_2O_{3(cr)}$	$Fe_2O_3 + 6H^+ + 2e^- \rightarrow 2Fe^{2+} + 3H_2O$	-75.71	-74.58	-73.49	-72.48	-71.52	-70.61	-69.71
sulfate	SO_4^{2-}	$SO_4^{2-} + 8e^- + 9H^+ \rightarrow HS^- + 4H_2O$	-23.08	-24.04	-25.12	-26.32	-27.61	-28.98	-30.45
CO_2 to methane	CO_2	$CO_2 + 8e^- + 8H^+ \rightarrow CH_4 + 2H_2O$	-15.04	-15.35	-15.72	-16.13	-16.59	-17.07	-17.59
CO_2 to acetate	CO_2	$2CO_2 + 8e^- + 7H^+ \rightarrow CH_3COO^- + 2H_2O$	-8.96	-8.97	-8.91	-8.80	-8.65	-8.46	-8.23
ED									
hydrogen	H_2	$H_2 \rightarrow 2H^+ + 2e^-$	-9.49	-8.86	-8.06	-7.11	-6.04	-4.85	-3.56
oxalate	$C_2HO_4^-$	$C_2HO_4^- + 2H_2O \rightarrow 3H^+ + 2HCO_3^- + 2e^-$	-1.67	-0.59	0.66	2.04	3.57	5.23	7.03
nucleotide, AMP^{2-}	$C_{10}H_{12}N_5O_7P^{2-}$	See * below	2.44	2.85	3.43	4.18	5.07	6.11	7.28
glucose	$C_6H_{12}O_6$	$C_6H_{12}O_6 + 12H_2O \rightarrow 6HCO_3^- + 24e^- + 30H^+$	9.55	10.02	10.62	11.34	12.18	13.12	14.16
ammonia	NH_3	$NH_3 \rightarrow 1/2N_2 + 3e^- + 3H^+$	11.41	11.93	12.42	12.90	13.38	13.87	14.38
amino acid, alanine	$C_3H_7NO_2$	$C_3H_7NO_2 + 7H_2O \rightarrow 3HCO_3^- + 14H^+ + NH_4^+ + 12e^-$	15.55	16.00	16.57	17.25	18.04	18.93	19.93
acetate	CH_3COO^-	$C_2H_3O_2^- + 4H_2O \rightarrow 9H^+ + 2HCO_3^- + 8e^-$	17.55	18.02	18.60	19.27	20.03	20.86	21.78
lipid *n*-alkane	$C_{16}H_{34}$	$C_{16}H_{34} + 48H_2O \rightarrow 16HCO_3^- + 114H^+ + 98e^-$	19.28	19.84	20.50	21.25	22.08	22.99	23.98
methane	CH_4	$CH_4 + 3H_2O \rightarrow 9H^+ + HCO_3^- + 8e^-$	19.33	19.88	20.57	21.37	22.27	23.27	24.37
Type III/IV kerogen	$C_{128}H_{68}O_7$	$C_{128}H_{68}O_7 + 377H_2O \rightarrow 694H^+ + 128HCO_3^- + 566e^-$	21.99	22.60	23.34	24.19	25.15	26.21	27.37
hydrogen sulfide	HS^-	$HS^- + 4H_2O \rightarrow SO_4^{2-} + 8e^- + 9H^+$	23.08	24.04	25.12	26.32	27.61	28.98	30.45
thiosulfate	$S_2O_3^{2-}$	$S_2O_3^{2-} + 5H_2O \rightarrow 2SO_4^{2-} + 8e^- + 10H^+$	26.36	27.45	28.71	30.12	31.67	33.34	35.14
sulfur	S^0	$S^0 + 4H_2O \rightarrow SO_4^{2-} + 6e^- + 8H^+$	32.94	34.04	35.36	36.85	38.50	40.29	42.24
ferrous iron	Fe(II)	$Fe^{2+} \rightarrow e^- + Fe^{3+}$	70.03	74.27	78.60	83.01	87.50	92.08	96.76
nitrite	NO_2^-	$NO_2^- + H_2O \rightarrow NO_3^- + 2e^- + 2H^+$	78.69	79.25	79.85	80.49	81.18	81.91	82.69
manganese	Mn^{2+}	$Mn^{2+} + 2H_2O \rightarrow MnO_2 + 4H^+ + 2e^-$	119.83	120.03	120.31	120.68	121.12	121.61	122.15

* $C_{10}H_{12}N_5O_7P^{2-} + 27H_2O \rightarrow 10HCO_3^- + 35H^+ + 5NH_4^+ + 30e^- + HPO_4^{2-}$; Calculated using revised-HKF equations of state (Helgeson and others, 1981; Tanger and Helgeson, 1988; and Shock and others, 1992), the SUPCRT92 software package (Johnson and others, 1992), and thermodynamic data taken from Shock and Helgeson, 1988; Shock and others, 1989; Shock and Helgeson, 1990; Sverjensky and others, 1997; Schulte and others, 2001; LaRowe and Helgeson, 2006; Helgeson and others 2009; and Snow and others, 2013

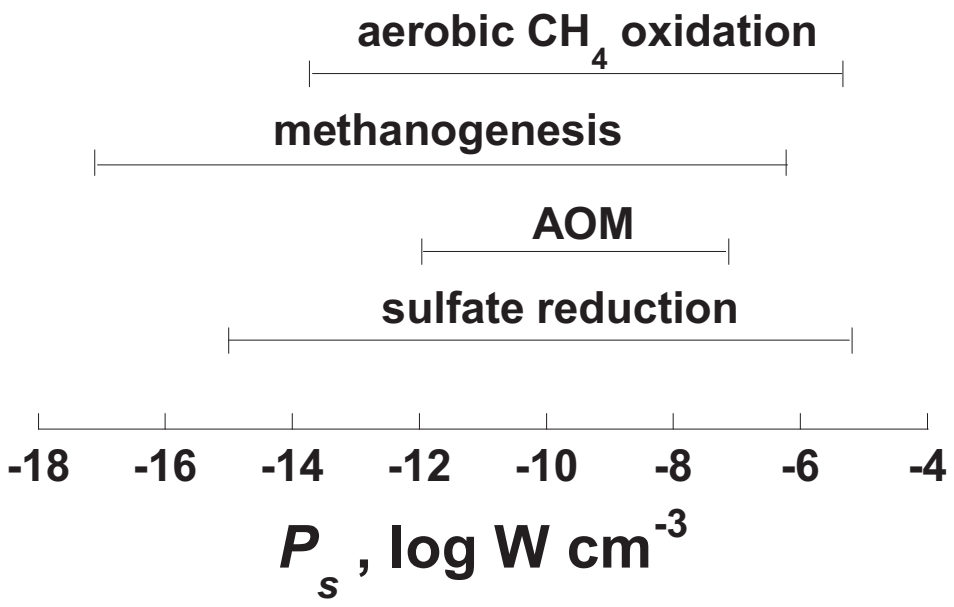

Fig. 1. Ranges of catabolic power, P_s, in the marine subsurface. These values were calculated from the catabolic reaction rates given in table 2 and the values of ΔG_r shown in table 4.

1993; Orcutt and others, 2005; Biddle and others, 2006; Joye and others, 2009; Omoregie and others, 2009), it isn't clear what percentage of cells are active. The amount of this power that is converted into new or refurbished cells is also unknown, but can be constrained using the approach discussed below.

The values of the Gibbs energies used to calculate the values of P_s listed in table 2 are reported in table 4 along with the reactions used to represent these processes and the activities of the reactants and products in these reactions. These activities are not

Table 4

Gibbs energies, (ΔG_r) of selected reactions

Reaction	ΔG_r	units
$4H_2 + SO_4^{2-} + H^+ \rightarrow HS^- + 4H_2O$	-154,684	J / mol SO_4^{2-}
$CH_3COO^- + SO_4^{2-} \rightarrow HS^- + 2HCO_3^-$	-84,675	J / mol SO_4^{2-}
$CH_4 + SO_4^{2-} \rightarrow HCO_3^- + HS^- + H_2O$	-42,933	J / mol CH_4
$4H_2 + HCO_3^- + H^+ \rightarrow CH_4 + 3H_2O$	-111,808	J / mol CH_4
$CH_3COO^- + H_2O \rightarrow CH_4 + HCO_3^-$	-41,720	J / mol CH_4
$CH_4 + 2O_2 \rightarrow HCO_3^- + H_2O + H^+$	-807,040	J / mol CH_4
$1/2O_2 + H_2$ v H_2O	-459,826	J / mol O_2
$CH_3COO^- + 4MnO_2 + 7H^+ \rightarrow 2HCO_3^- + 4Mn^{2+} + 4H_2O$	-236,774	J /mol Mn^{2+}

Conditions: T = 25 °C, P = 250 bars; activities are $H_2 = 10^{-4}$, $SO_4^{2-} = 0.01$, $HS^- = 10^{-6}$, pH = 7, $CH3COO^- = 0.001$, $HCO_3^- = 0.002$, $O_2 = 0.00015$, $CH_4 = 10^{-5}$, $Mn^{2+} = 10^{-6}$.

See Appendix for computational methods.

specific to the locations for which reaction rates have been determined, but are nominal values used to illustrate the range of power supplies existing in marine settings due to the variation in reaction rates. As is discussed and quantified below, the activities of the species in these reactions can vary substantially from one environment, thereby altering values of ΔG_r. However, the data required to accurately determine values of activity—temperature, pressure, ionic strength and the concentrations of all species in the reaction—are not available for most of the sites summarized in table 2.

Dissipated Catabolic Power

Only a portion of catabolic power is used to generate biomass. The remainder is used for any number of cellular activities including shifts in metabolic pathways, energy spilling reactions, cell motility, changes in stored polymeric carbon, osmoregulation, extracellular secretions, defense against chemical stresses and the "proofreading", synthesis and turnover of macromolecules such as proteins and RNA (van Bodegom, 2007). These non-growth activities are sometimes referred to collectively as maintenance or as costing microorganisms a certain amount of maintenance energy. Values of maintenance energies that have been reported in the literature, summarized below, are typically determined under relatively high-energy conditions (Hoehler and Jørgensen, 2013). As a result, these maintenance values represent the energy that is not used for growth while the organisms are experiencing rather luxuriant conditions that may not be very representative of natural settings. One could think of such maintenance energies as the upper limit for microbial power usage that does not result in growth, that is, rather wasteful energy dissipation. On the other end of the maintenance energy spectrum is the basal power requirement, which has been defined as "the energy flux associated with the minimal complement of functions required to sustain a metabolically active state" (Hoehler and Jørgensen, 2013). Effectively, the basal maintenance power is relevant for the activity levels of microorganism in low-energy, natural environments, which are common in the subsurface. If values of the basal power requirement were known, then it would be a simple task to determine how many microorganisms can be sustained in a given ecosystem from particular catabolic reactions. In the absence of such data, it is instructive to mine the maintenance energy/power literature to begin to develop methods for quantifying the relationship between the supply of power in a given environment and the number and type of microorganisms that can be supported in it.

Many studies have attempted to quantify maintenance energy/power to determine how much energy microorganisms use for purposes other than growth (see review by van Bodegom, 2007). However, the formulations used to do so contain variables (for example, growth yield, relative growth rates and death rates) that are treated as constants (van Bodegom, 2007) resulting in poor predicative capabilities when growth rates are low; even predicting substrate utilization when the substrate concentrations are 0, (Pirt, 1987). In addition, it has been shown that maintenance coefficients depend on growth conditions (Neijssel and Tempest, 1976; Chesbro and others, 1979; Goma and others, 1979; Beyeler and others, 1984), and therefore should be captured by a variable, not a constant. Furthermore, models that define a maintenance supply (Schulze and Lipe, 1964) or maintenance coefficient (Pirt, 1965) as the minimum substrate consumption to maintain a cell ignore the fact that the amount of energy that can be supplied by a single substrate (generally defined as the electron donor) depends strongly on the identity and concentration of the complementary electron acceptor and the temperature, pressure and composition of the environment.

In order to remedy these shortcomings, van Bodegom (2007) proposes a new formulation for a single maintenance coefficient that encompasses all energy expenditures that do not lead to growth. However, this model may be prohibitively complex for application to natural systems. It requires an abundance of organism-specific informa-

TABLE 5

Selected values of cell-specific maintenance power requirements, P_{cs}

Metabolism	Organism	Maintenance power requirement P_{cs}, fW /cell	Reference
Anoxygenic phototrophy	*Rhodobacter capsulatus* KB1	93	Marschall and others (2010)
	chemoorganoheterophic bacteria	5.3 - 7.2	Marschall and others (2010)
Anoxygenic phototrophy	*Chlorobium* phylotype BS-1	0.019 - 0 .057	Marschall and others (2010)
photoheterotrophy	marine bacteria	2.3 - 4.6	Kirchman and Hanson (2013)
(propionate, organics) + (sulfate, fumarate)	*Syntrophobacter fumaroxidans*	0.32	Marschall and others (2010)
SO_4^{2-} + lactate	*Desulfovibrio desulfricans*	44[a]	Okabe and others (1992)
Sulfate reduction	*Desulfovibrio vulgaris*	110[c]	Tijhuis and others (1993)
Thermophilic anaerobes		7.8 - 28[b]	Rinker and Kelly (2000)
Anaerobes		0.36 - 8.6[b]	Rinker and Kelly (2000)
Aerobic heterotrophy		49 - 4700[c]	Tijhuis and others (1993)
$O_2 + S_2O_3^{2-}$		120 - 1900[c]	Tijhuis and others (1993)
$O_2 + NH_4^+$		28[c]	Tijhuis and others (1993)
Fermentation	*Syntrophobacter fumaroxidans*	0.15[c]	Scholten and Conrad (2000)
Fermentation		6.4 - 260[c]	Tijhuis and others (1993)
$4H_2 + CO_2 \rightarrow CH_4 + 2H_2O$		1400 -1600[c]	Tijhuis and others (1993)

[a]assuming −170 kJ/mol lactate, 86 fg/dry cell; [b]assuming −150 kJ/mol OM, 86 fg/dry cell; [c]assuming 86 fg C/cell.

tion such as the maximum relative growth rate, growth rate of the active fraction of the population, a yield coefficient corrected for maintenance, a maintenance coefficient for excretion, leakage and cell death and the substrate consumption for physiological maintenance per increment of biomass change. There is no organism for which all—or even a majority—of these constants are known. Furthermore, this and all other maintenance models are suited to model organisms growing under laboratory conditions, that is, relatively high energy, nutrient replete and short timescales. Not only are there massive differences between microbial growth rates in the laboratory and in natural settings (LaRowe and others, 2012), but in deep settings, metabolic rates can be at least 4 orders of magnitude lower than in surface samples (Price and Sowers, 2004) and per-cell energy fluxes appear to be several orders of magnitude lower than maintenance energies predicted from laboratory cultures (Jorgensen, 2012). Nonetheless, maintenance energies reported in the literature can be viewed as the high end of the spectrum quantifying the amount of energy that microorganisms use for purposes other than growth.

Maintenance power requirement.—Values of the maintenance power requirements for a number of microbial metabolisms, including photosynthesis, sulfate reduction, fermentation and a variety of aerobic processes, are summarized in table 5. All of these values have been converted into units of specific power (fW cell^{-1}). Per-cell values range over more than 5 orders of magnitude, from 0.019 fW for an anaoxygenic phototroph to 4700 fW for aerobic heterotrophy. There are no clear cut patterns relating metabolic pathway to maintenance power requirements. For instance, maintenance power requirements for hydrogenotrophic methanogenesis are among the highest (1400 − 1600 fW cell^{-1}), aerobic metabolism varies between 28 and 4700 fW cell^{-1}, fermentation ranges from 0.15 to 260 fW cell^{-1} and photosynthesis falls between 0.019 to 93 fW cell^{-1}. It should be noted that most of the values given in table 5 are based on standard state values of Gibbs energies of reaction (ΔG_r^0) and not, as should be done, on ΔG_r.

Although the variability in table 5 suggests how difficult it would be to assign accurate values of cellular power demand in natural settings, the concept of power dissipation is still useful for determining growth rates. Given cell-specific maintenance power requirement, P_{cs}, the total catabolic power dissipated in a cm^3 of sediment or fluid is simply the product of P_{cs} and the size of the active microbial population in that cm^3:

$$P_d = |P_{cs}| \cdot B_j \tag{2}$$

where P_d refers to catabolic power that is dissipated (that is, does not result in new biomass) and B_j refers to the number of active cells catalyzing the jth reaction per cm^3. By taking this approach, there are now two simple statements, equations (1) and (2), describing the catabolic power available in an environment and the amount of this power that is *not* used to synthesize biomolecules. Calculating the power that is dissipated (P_d) avoids the virtually impossible task of summing up all of the non-biosynthetic metabolic processes noted above that consume catabolic power, including inefficiencies and waste, and how these processes vary among different organisms and from one environment to another. This is especially daunting given that the vast majority of microorganisms have not been and may never be cultured in the laboratory. A logical consequence of this model is that when $P_s > P_d$, growth, or at least biomolecular replacement, can ensue. Conversely, when $P_s < P_d$, the population size, or total biomass, shrinks, or the percentage of metabolically active cells decreases. The magnitude of growth arising from catabolic power is determined by quantifying the cost of synthesizing biomolecules, expressed as a biomass yield.

Yield

The catabolic power that is used to synthesize new cells or replace cellular components can be converted into common biomass units (cell cm^{-3}) by using a yield term. Biomass yield, Y, is typically defined as the number of cells (or quantity of cellular carbon or protein) generated from a given mass of substrate. Although values of Y are often treated as constants for a particular organism or metabolic pathway, Y is known to vary as a function of growth rate and other variables (van Bodegom, 2007). The variability of Y is illustrated in table 6. Here, values of Y for many different catabolic activities are listed. It can be seen that Y (in g cells/mol substance) varies from 0.3 for aerobic oxidation of nitrite to 88 for aerobic heterotrophy. Yield values are 1.6 to 15 for nitrate reduction, 14 to 62 for fermentation and 0.6 to 8.7 for methanogenesis. Yield values for methanotrophy apparently vary by a factor of 40, depending on whether it occurs in sediments, peat, tundra soils, landfills or the laboratory (Segers, 1998). Clearly, the amount of biomass that can be produced from a mole of substrate depends acutely on the nature of the environment in which it is happening. Furthermore, it should be noted that the values of Y shown in table 6 are likely maximum yield values since the experiments carried out to determine them were designed to optimize biomass production. In order to take environmental factors into account, the yield term used in this communication is based on the Gibbs energy of synthesizing biomolecules in the environment of interest. Although a number of models have been developed that seek to link biomass production to various energetic parameters, a new model is introduced here that accounts for environmental variables and the type of metabolism. In order to provide context for this new model, previous efforts are summarized first.

A brief review of yield models.—Numerous studies have proposed methods to predict biomass yields using energetic parameters. These models employ a number of different approaches that link biomass yield to: ATP production, the number of electrons available in the organic carbon that is oxidized, the ratio of electrons conserved in

TABLE 6

Selected values of biomass yield coefficients, Y, for exponentially growing cells

Electron acceptor	Reaction or Process	Yield (g cells/mol substrate)	Reference
O_2	waste water & pharmaceutical waste:		
	nitrification	0.51 -3.6	Gupta and Sharma (1996)
	heterotrophy	22 - 47[a]	Gupta and Sharma (1996)
	$CH_4 + O_2 \rightarrow CO_2 + 2H_2O$	10[b]	Dale and others (2010)
	$2O_2 + H_2S \rightarrow SO_4^{2-} + 2H^+$	10[b]	Dale and others (2010)
	carbohydrate + O_2	88[c]	Rittman and McCarty (2001)
	organic matter + O2	43[a]	Rittman and McCarty (2001)
	$NO_2^- + 1/2O_2 \rightarrow NO_3^-$ by Nitrospira	2.1	Blackburne and others (2007)
	$NO_2^- + 1/2O_2 \rightarrow NO_3^-$ by Nitrobacter	0.3	Blackburne and others (2007)
	$NO_2^- + 1/2O_2 \rightarrow NO_3^-$	4	Rittman and McCarty (2001)
NO_3^-/NO_2^-	anaerobic sulfide oxidation	10	Dale and others (2010)
	$H_2 + NO_3^-$	1.6	Rittman and McCarty (2001)
	$S^0 + NO_3^-$	4.8	Rittman and McCarty (2001)
	organic matter + NO_3^-	15[a]	Rittman and McCarty (2001)
SO_4^{2-}	SO_4^{2-} + lactate, *Desulfovibrio desulfuricans*	1.5 - 1.6	Okabe and others (1992)
	SO_4^{2-} + acetate	3.4	Rittman and McCarty (2001)
	$SO_4^{2-} + H_2$, *Desulfovibrio* G11	2.8 - 4.0[d]	Robinson and Tiedje (1984)
Fermentation	sugar	23[c]	Rittman and McCarty (2001)
	maltose/glucose, *Thermotoga maritima*	14 - 45	Rinker and Kelly (2000)
	maltose, *Pyrococcus furiosus*	26-50	Rinker and Kelly (2000)
	glucose, *Thermoanaerobium brockii*	50	Rinker and Kelly (2000)
	glucose	21-62	Rinker and Kelly (2000)

TABLE 6
(Continued)

Electron acceptor	Reaction or Process	Yield (g cells/mol substrate)	Reference
Methanogenesis	$4H_2 + CO_2 \rightarrow CH_4 + 2H_2O$		Rittman and McCarty (2001)
	$4H_2 + CO_2 \rightarrow CH_4 + 2H_2O$	0.6-6.4	Daniels and others (1984)
	$4H_2 + CO_2 \rightarrow CH_4 + 2H_2O$, *Methanothermobacter thermautotrophicus:* 12, 80 kPa H_2	3, 7	De Poorter and others (2007)
	$4H_2 + CO_2 \rightarrow CH_4 + 2H_2O$	0.6 - 8.7	De Poorter and others (2007)
	$4H_2 + CO_2 \rightarrow CH_4 + 2H_2O$, *M. hungatei* JF-1	0.64 - 1.0[d]	Robinson and Tiedje (1984)
	$CH_3COO^- + H^+ \rightarrow CH_4 + CO_2$	2.1	Rittman and McCarty (2001)
	$CH_3COO^- + H^+ \rightarrow CH_4 + CO_2$, *Methanosarcina*	2.1	Jetten and others (1992)
	$CH_3COO^- + H^+ \rightarrow CH_4 + CO_2$, *Methanothrix*	1.4	Jetten and others (1992)
	$CH_3COO^- + H^+ \rightarrow CH_4 + CO_2$	1.1-3.1	Daniels and others (1984)
	$4HCOO^- + 4H^+ \rightarrow CH_4 + 3CO_2 + 2H_2O$	4.8-5.8	Daniels and others (1984)
	$*CH_3OH \rightarrow CH_4$	4.1-6	Daniels and others (1984)
	$4CH_3NH_2 + 2H_2O \rightarrow 3CH_4 + CO_2 + 4NH_3$	6	Daniels and others (1984)
Miscellaneous	Anammox, $NH_4^+ + NO_2^- \rightarrow N_2 + 2H_2O$	2.2	Strous and others (1999)
	Methanotropy: compilation from isolates, fresh sediments, peat, tundra soils and landfills	0.5 - 20[b]	Segers (1998)
	Propionate fermentation (synthrophic) *Syntrophobacter fumaroxidans*	2.6	Scholten and Conrad (2000)
	Propionate + SO_4^{2-} (synthrophic) *Syntrophobacter fumaroxidans*	0.82 -1.24	Scholten and Conrad (2000)
	$4H_2 + CO_2 \rightarrow CH_4 + 2H_2O$, synthrophic, *M. hungatei*	7.6	Scholten and Conrad (2000)
	Anaerobic methane oxidation	0.6	Nauhaus and others (2007)

[a]acetate used; [b]biomass taken to be $C_5H_7O_2N$ (Rittmann and McCarty, 2001); [c]glucose used; [d]assumed protein is half the weight of a dry cell; *methanol can be reduced to methane or disproportionated to methane and CO_2.

biomass to the amount of electrons available in an organic substrate by aerobic combustion to HCO_3^-, the number of moles of carbon in the processed substrate, the ratio of Gibbs energies associated with the sum of consumed substances to produced substances, the Gibbs energy of converting inorganic precursors into biomass and the energy of fully carrying out a catabolic reaction, and the ratio of anabolism to catabolism and enthalpy efficiencies (Heijnen and van Dijken, 1992). All of these formulations are thoroughly reviewed by Heijnen and van Dijken (1992), who conclude that their range of applicability is very limited since many are not thermodynamically grounded (for example, some potentially violate the 2nd law of thermodynamics and others use over-defined reference states) and/or require detailed but rarely available biochemical information about the metabolic pathways used. To rectify the situation, the same authors propose a similar method to find a yield correlation based on the Gibbs energy of catabolism. However, the correlation developed in Heijnen and van Dijken (1992), which is more expansive than those summarized above, uses only standard state values of the Gibbs energy of reaction, is restricted to the reference state of pH 7 and 25 °C, considers only C_1-C_6 carbon compounds, does not take pressure into account and the only electron acceptors considered are oxygen and nitrate, although fermentation is also included. They report yield coefficients ranging from 250 to 3500 kJ (mol dry biomass C)$^{-1}$. More recently, (Liu and others, 2007) used a similar approach, and essentially the same data set, to correlate biomass yield and energetics. Their model is a simplified version of the one described by Heijnen and van Dijken (1992) and also only uses standard state Gibbs energies. Despite noting the range of values reported by Heijnen and van Dijken (1992), Liu and others (2007) assert that a yield of 500 kJ (mol dry biomass C)$^{-1}$ is sufficient to represent all microorganisms.

The yield coefficients that are based on standard state Gibbs energies share the same shortcoming as those that relate grams of biomass produced per mole or gram of substrate: neither approach takes into account the diversity of natural habitats. In particular, the amount of energy available per mole of a given substrate can vary substantially from one environment to another, especially when comparing the laboratory to the deep biosphere, where most microorganisms exist under very lower energy states (Jørgensen and D'Hondt, 2006; Jørgensen and Boetius, 2007; Jørgensen, 2012). For example, values of ΔG_r for sulfate reduction coupled to H_2 oxidation as a function of temperature are shown under different environmental conditions (different concentrations of reactants and products) in figure 2A. From 0 to 125°C, the Gibbs energies of H_2 oxidation by sulfate can flip from endergonic to exergonic, yielding as much as 200 kJ per mole of SO_4^{2-} (shaded region). A yield coefficient obtained under high energy conditions for this reaction would grossly misrepresent the amount of energy, and thus the biomass yield, that hydrogenotrophic sulfate reducing organisms could obtain under less favorable conditions. The energetic biomass yield values that are based on ΔG_r^0, standard state values Gibbs energies (Heijnen and van Dijken, 1992; Liu and others, 2007), can be even less representative than those measured under high energy conditions. Note in figure 2A that for $SO_4^{2-} + H_2$, ΔG_r^0 (dashed line) differs from ΔG_r (shaded region) by ~50 to > 300 kJ (mol of SO_4^{2-})$^{-1}$ at the conditions of interest. Although less demonstrably so, the same is true for other catabolic reactions. This is shown in figures 2B and 2C, respectively, for sulfate reduction coupled to acetate and methane oxidation. Again, the shaded regions represent the ranges of ΔG_r based on different concentrations of reactants and products in these reactions and the dashed lines represent ΔG_r^0 for the indicated reactions.

Using a fixed value for biomass yield would predict the same amount of biomass produced by organisms catalyzing the same reaction in two very different environments, despite the large difference in energy availability in these settings. The reaction

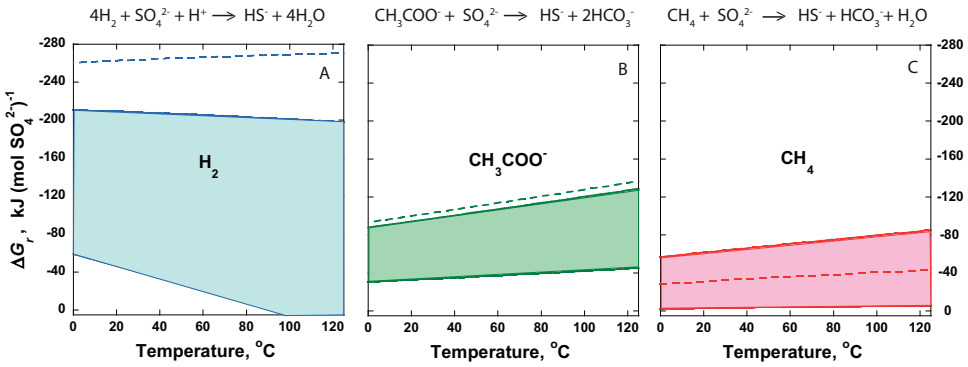

Fig. 2. Gibbs energies, ΔG_r, of sulfate reduction coupled to (A) H_2, (B) acetate (CH_3COO^-) and (C) CH_4 oxidation under high and low energy conditions as a function of temperature. The activities used in these calculations are as follows: Low energy conditions (lower lines of shaded regions), $SO_4^{2-} = 10^{-4}$, $HS^- = 0.01$, $HCO_3^- = 0.002$, $H_2 = 10^{-7}$, $CH_3COO^- = 10^{-6}$, CH4 $=10^{-6}$ pH = 8.5 and for the high energy calculations (upper lines of shaded regions), $SO_4^{2-} = 0.03$, $HS^- = 10^{-6}$, $HCO_3^- = 0.002$, $H_2 = 0.01$, $CH_3COO^- = 0.01$, $CH_4 = 10^{-2}$ and pH = 6. The dashed lines refer to standard state values of the Gibbs energy of these reactions.

of interest could even be endergonic in the environment under study, but a fixed yield value would predict an increase in biomass. Furthermore, the amount of energy available in an environment from a catabolic reaction does not sufficiently define the amount of biomass that can be sustained in it. It is the rate at which this energy is used, the power, and the rate at which it is dissipated that defines the potential of an environment for hosting microorganisms. Perhaps because so many of the studies summarized in table 6 are directed towards optimizing the industrial application of microorganisms, there is little to no focus on how environmentally relevant variables affect these yield values. In an effort to take these factors into account, the following method for computing biomass yield has been developed.

Calculating biomass yield.—The approach adopted in the current study for calculating biomass yield combines the ΔG_r of biomolecule synthesis, catabolic power supply (P_s) and the proportion of P_s that does not result in new biomass (P_d). The change in biomass as a function of time, $\frac{dB_j}{dt}$, can be summarized as a combination of equations (1) and (2) and a yield coefficient, Y (cells J^{-1}):

$$\frac{dB_j}{dt} = Y_j\left(\left|\frac{\Delta G_r}{\nu_i}\right|\cdot r_j - |P_{cs}|\cdot B_j\right) \tag{3}$$

or in a simplified form as

$$\frac{dB_j}{dt} = Y_j(P_s - P_d) \tag{4}$$

Equation (3) relates biomass change to the rate and energetics of catabolism while taking into account the amount of this power that is not used for increases in biomass, P_d. Values of P_d can be computed using equation (2), cell counts and the values of P_{cs} given in table 5, or by assuming that it is a particular percentage of the catabolic power supply (see below). The latter constraint can be thought of as a declaration of the efficiency with which organisms convert power into biomass. As noted above, when values of P_d exceed those of P_s, the size of the active bacterial population shrinks. In this

case, the yield coefficient loses its meaning, and the number of microorganisms that can remain active for a given power supply is simply calculated using

$$B_j = \frac{P_s}{P_{cs}} \tag{5}$$

Unmet maintenance power needs could be due to a hostile environment, sluggish catalysis rates under low energy conditions or some combination of these factors. In the case of biomass loss due to other factors such as predation or the accumulation of toxic, lysogenic compounds, an additional term can be added to equation (4) to account for this,

$$\frac{dB_j}{dt} = Y_j(P_s - P_d) - DB_j \tag{6}$$

where D stands for a decay constant that would be characteristic of a particular process, in units of sec^{-1}. It should be noted that although biomass concentrations in units of cell cm^{-3} are used in this study, equations (3), (4) and (5) can be used to model populations of microorganisms that are attached to surfaces or living in biofilms as well. In this case, the units for r, B_j and $\frac{dB_j}{dt}$ are recast in terms of surface area: r becomes mol cm^{-2} sec^{-1}; B_j, cell cm^{-2}; $\frac{dB_j}{dt}$, cell cm^{-2} sec^{-1}. Unlike the yield formulations reviewed above, values of Y_j in equations (3), (4) and (6) are not static, but a function of the environment. They are calculated as follows.

Calculating biomass yield coefficients, Y.—The yield coefficients, Y, that describe the amount of biomass that can be made from a given amount of substrate are not fixed, but a function of the variables that describe the environment where growth is occurring. In addition to the variable energetics of anabolism, the amount of biomass required to make a cell can vary depending on the setting. In this section, a method for determining values of biomass yield coefficients is presented in addition to several values of Y under specified conditions. Values of yield coefficients are calculated using in units of (cells J^{-1}) using

$$Y = \left(\frac{\text{gram bio}}{\text{J}}\right)\left(\frac{\text{cells}}{\text{gram bio}}\right) \tag{7}$$

where values of $\left(\frac{\text{gram bio}}{\text{J}}\right)$, the mass of dry cells that can be made from a Joule of Gibbs energy, are determined as define below. Values of the second term on the right hand side of equation (7), the number of cells in a dry gram of biomass, $\left(\frac{\text{cells}}{\text{gram bio}}\right)$, are calculated from

$$\left(\frac{\text{cells}}{\text{gram bio}}\right) = \left(\frac{\text{cells}}{\text{gram C}}\right)\left(\frac{\text{mol bio}}{\text{gram bio}}\right)\left(\frac{\text{mol C}}{\text{mol bio}}\right)\left(\frac{\text{gram C}}{\text{mol C}}\right) \tag{8}$$

where $\left(\frac{\text{cells}}{\text{gram C}}\right)$ is the inverse of the numbers of grams of carbon in a cell, a value sometimes reported in the literature. The number of moles of biomass per gram of biomass, $\left(\frac{\text{mol bio}}{\text{gram bio}}\right)$, and the moles of C per mole of biomass, $\left(\frac{\text{mol C}}{\text{mol bio}}\right)$, are assumed

to be (1/113.1146) and 0.2, values taken from the stoichiometry of microbial organisms: $C_5H_7O_2N$ (Rittman and McCarty, 2001). The number of grams of carbon in a non-eukaryotic cell is known to vary between, at least, 4 and 86 fg (Kallmeyer and others, 2012), so values of $\left(\frac{\text{cells}}{\text{gram bio}}\right)$, as calculated using equation (8) can in turn range from 1.3×10^{14} and 6.2×10^{12} cells per dry gram of biomass.

Calculating values of $\left(\frac{\text{gram bio}}{\text{J}}\right)$, the first term on the right hand side of equation (7), is a more complicated endeavor. The procedure used to do so involves summing values of ΔG_r for synthesizing all of the biomolecules that make up a dry gram of prokaryotic cells under the environmental conditions of interest:

$$\left(\frac{\text{gram bio}}{\text{J}}\right) = \left(\sum_i (\Delta G_{r,i})\left(\frac{\text{mol } i}{\text{gram cell}}\right) + \Delta G_{r,\text{ polym}}\right)^{-1} \tag{9}$$

where $\Delta G_{r,i}$ stands for the Gibbs energy of synthesizing the ith biomolecule, J mol^{-1}, $\left(\frac{\text{mol } i}{\text{gram cell}}\right)$ represents the number of moles of biomolecule i in a dry gram of bacterial cells and $\Delta G_{r,\text{polym}}$ refers to the Gibbs energy of polymerizing all of the biopolymers in a dry gram of cells. All three of the terms of on the right-hand side of equation (9) can vary with the type and size of cells present, the sources of carbon, nitrogen and sulfur needed to synthesize biomolecules and the temperature, pressures and composition of the environment of interest. In order to simplify the application of equation (9), and therefore the procedure for calculating values of yield coefficients, the following assumptions have been made.

The number of moles of biomolecules in a gram of dry biomass, $\left(\frac{\text{mol } i}{\text{gram cell}}\right)$, are taken from (Battley, 1991), which uses *E. coli* as a model bacterium. Values of $\Delta G_{r,i}$ required to evaluate equation (9) are taken from (McCollom and Amend, 2005), but modified for the revised thermodynamics properties of methionine (LaRowe and Dick, 2012). The energy required to polymerize all the biomacromolecules that constitute a dry gram of microbial cells, $\Delta G_{r,\text{polym}}$, were calculated using the energy that it takes to polymerize all of the polypeptides in a dry gram of cells, 191 J (g cells)$^{-1}$, (Amend and others, 2013), and the following assumptions. Since 55 percent of the dry weight of a bacterial cell (*E. coli*) is protein and 32 percent of the remaining mass is also biopolymers [20.5% RNA, 3.1% DNA, 3.4% lipopolysaccharides, 2.5% peptidoglycan and 2.5% glycogen (Battley, 1991)], it was assumed that the energy required to produce polypeptides from amino acids is proportional to that for polymerizing the other biomacromolecules. This is based on the fact that biopolymerization reactions are dehydration reactions, the energetics of which should not change much from one environment to the next. That is, if 191 Joules is required to polymerize all the protein in a dry gram of cells, protein comprises 55 percent of the dry weight of a single cell and 32 percent of the rest of the dry weight is other polymers, then 111 J (g cells)$^{-1}$ = ((32/55)·191 J (g cells)$^{-1}$) is required to polymerize all the RNA, DNA, lipopolysaccharides, peptidoglycan and glycogen in a cell. Summing the energy required to polymerize protein plus all of these other polymers yields $\Delta G_{r,\text{polym}}$, 302 J (g cells)$^{-1}$.

In order to illustrate how environmental conditions influence values of yield coefficients, several computed values of Y are listed in table 7. These values have been generated using equations (7-9) and fixed values of $\left(\frac{\text{mol } i}{\text{gram cell}}\right)$ (see (Battley, 1991), the number of grams of carbon in a cell, 65 fg C/cell (Hoehler and Jørgensen, 2013)

TABLE 7

Energy-based yield coefficients, Y, in units of cells J^{-1}

		Nitrogen and sulfur sources	
redox state	**mV**	**NH_4^+, HS^-**	**NO_3^-, SO_4^{2-}**
microaerophilic	77	4.40 x 10^8	3.76 x 10^8
reducing	-27	4.67 x 10^9	1.66 x 10^9

In all cases, 8.2×10^{12} cells per gram of biomass was assumed and the sources of C and P are HCO_3^- and HPO_4^{2-}.

or 8.2×10^{12} cells per dry gram of biomass, $\left(\frac{\text{cells}}{\text{gram bio}}\right)$, and $\Delta G_{r,\text{polym}} = 302$ J (g cells)$^{-1}$ under two redox conditions for different sources of carbon, nitrogen and sulfur. By specifying values of these variables, the remaining contributing factor influencing the values of *Y* depicted in table 7 is the number of grams of biomass that can be produced per Joule.

The values of $\left(\frac{\text{gram bio}}{\text{J}}\right)$ used with equation (7) to generate the yield coefficients listed in table 7 under microaerophilic (+77 mV) and reducing (−27 mV) conditions are 5.37×10^{-5} and 5.70×10^{-4} grams of biomass per Joule. These values were calculated using equation (9), the fixed values of $\left(\frac{\text{mol } i}{\text{gram cell}}\right)$ and $\Delta G_{r,\text{polym}}$ noted above and values of the Gibbs energy of synthesizing the *i*th biomolecule, $\Delta G_{r,i}$, taken from and McCollom and Amend (2005) and slightly modified in order to account for the significantly revised thermodynamic properties of methionine (LaRowe and Dick, 2012). That is, McCollom and Amend (2005) reported the first term on the right hand side of equation (9), $\sum_i (\Delta G_{r,i})\left(\frac{\text{mol } i}{\text{gram cell}}\right)$, equal to 18,435 and 1,434 J (g cells)$^{-1}$ under microaerophilic (+77 mV) and reducing (−27 mV) conditions, respectively. The revised values used here are 18,318 and 1,452 J (g cells)$^{-1}$. It should be noted that these refer to the energetics of biomonomer synthesis reactions written using HCO_3^-, NH_4^+, HS^- and HPO_4^{2-} as the respective sources of C, N, S and P. If the sources of nitrogen and sulfur used to synthesize biomolecules are NO_3^- and SO_4^{2-}, rather than NH_4^+ and H_2S, then an additional 3,170 J is required to make all the monomers in dry gram of cells. In this case, values of $\left(\frac{\text{gram bio}}{\text{J}}\right)$ become 4.59×10^{-5} and 2.03×10^{-4} grams of biomass per Joule.

It should be emphasized that the energy required to synthesize biomolecules from inorganic precursors and polymerized into biopolymers used to calculate the values of *Y* shown in table 7 only account for the direct cost of making these compounds from specified inorganic precursors. Inefficiencies associated with particular biosynthetic pathways, enzyme synthesis, nutrient acquisition and other energy-demanding processes, which are difficult to quantify in natural settings, are excluded. Furthermore, the values of *Y* are, strictly speaking, only relevant to 25 °C and 1 bar and do not account for the full range of precursor molecules such as acetate or other organics serving as the carbon source. However, variations in redox potential, which are emphasized in table 7, are far larger contributors to variations in *Y* than the sensitivity of monomer synthesis and polymerization to different temperatures and pressures

(see Amend and Shock, 1998; LaRowe and Regnier, 2008; LaRowe and Dick, 2012; Amend and others, 2013).

The energy-based values of Y reported by Liu and others (2007) and Heijnen and van Dijken (1992), which are given in units of kJ (dry mol C_{bio})$^{-1}$ can be converted to the same units as the yield coefficients reported in table 7 using

$$\left(\frac{\text{cells}}{\text{J}}\right) = \left(\frac{\text{dry mol C}_{\text{bio}}}{\text{J}}\right)\left(\frac{\text{1 mol bio}}{\text{5 mol C}_{\text{bio}}}\right)\left(\frac{\text{grams bio}}{\text{mol bio}}\right)\left(\frac{\text{cells}}{\text{grams bio}}\right) \tag{10}$$

and assuming that biomass can be represented as $C_5H_7O_2N$ and that each cell contains 65 fg C (see above). The values, 250, 500 and 3500 kJ (dry mol C_{bio})$^{-1}$ reported by Liu and others (2007) and Heijnen and van Dijken (1992) become 7.4×10^8, 3.7×10^8 and 5.3×10^7 cell J^{-1}, which are similar to yield coefficients calculated in this study for microaerophilic conditions. In fact, the value of Y corresponding to 500 kJ (dry mol C_{bio})$^{-1}$ is virtually identical to Y calculated for microaerophilic conditions when the sources of C, N, S and P are HCO_3^-, NH_4^+, HS^- and HPO_4^{2-}, 3.7×10^8 versus 3.76×10^8 cells J^{-1}. The larger values of Y shown in table 7 for reducing conditions are 6 to 2 times larger than the highest yield values reported by (Heijnen and van Dijken, 1992), depending on the sources of N and S, respectively.

APPLICATIONS OF THE BIOMASS EQUATION OF STATE

The equations presented above can be used to constrain the growth/replacement rates of microorganisms in natural settings and the proportion of microbial populations that are active in a given environment. Several demonstrations of the utility of these equations are presented below.

Maintaining Population Sizes

In order to gain an understanding of how many microbial cells can be sustained in a given environment, values of biomass, B, in units of cells cm^{-3} are plotted in figure 3 as a function of maintenance power. In particular, values of B are plotted as a function of catabolic power, P_s, for different values of cell-specific maintenance powers, P_{cs}. The range of P_s considered spans that of the values tabulated in table 2 and those for P_{cs} include the range given in table 5, the shaded area, and several orders of magnitude above and below this. It can be seen in figure 3 that the number of cells that can be supported in a setting from a particular amount of power can vary substantially based on how much power is channeled into biomass synthesis. For instance, at $P_s = 10^{-10}$ W cm^{-3}, a population of 10 to nearly 10^8 cells could be supported for the range of maintenance power demands reported in the literature. If organisms have basal power requirements several orders of magnitude lower than what has been observed in the laboratory (for example, 10^{-20} W cell^{-1}), then a low power supply of, for example, 10^{-15} W cm^{-3} could support a community of about 10^5 cells.

Although values of P_{cs} have been specified to construct figure 3, equation (5) can be used in conjunction with cell counts, reaction rates and Gibbs energies of reactions to place limits on the average amount of power that is required to sustain microorganisms in particular environments such as the deep subsurface. As long as sufficient geochemical data are reported for a site, values of ΔG_r can be readily calculated, and reaction rates can be modeled using reaction transport models if they are not measured directly. That is, values of cell-specific basal maintenance powers can be calculated from geochemical information and equation (5).

Doubling/Replacement Times

Upon integration, equation (4) can be used to calculate how the size of a microbial population changes as a function of energy availability and time, $B_{j,t}$:

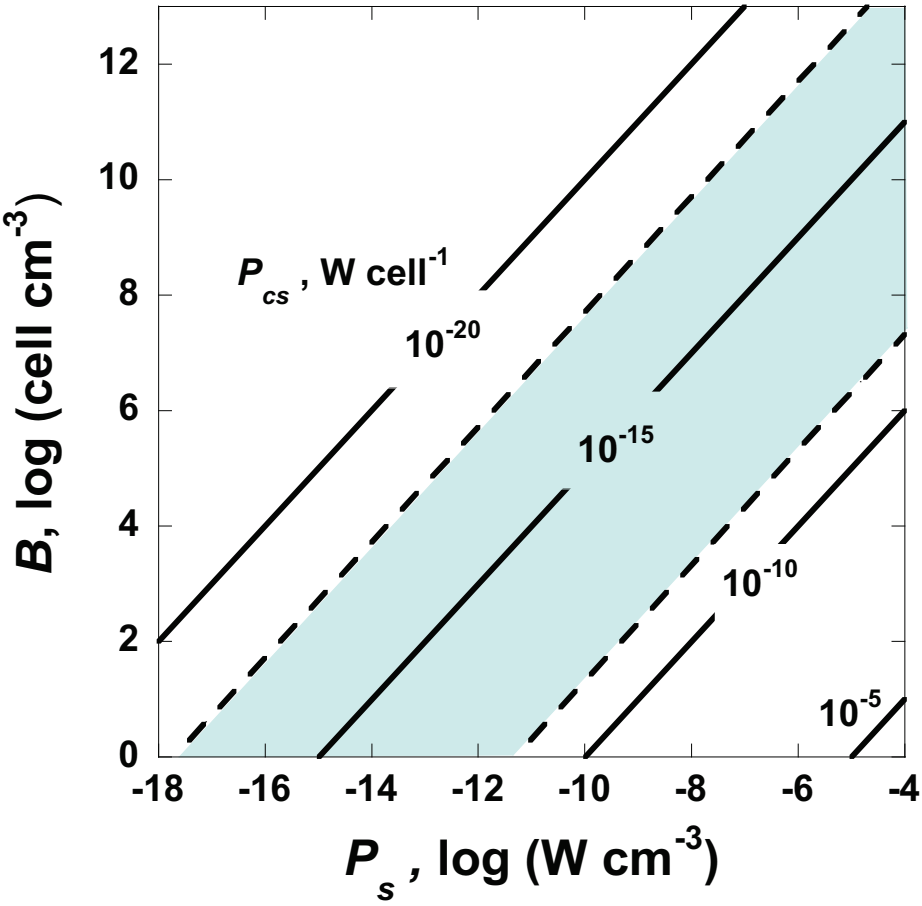

Fig. 3. Biomass concentrations that can be supported in a cm^3 of sediment over the range of values of catabolic power supply, P_s, shown in figure 1 and listed in table 2 for a selection of single cell maintenance powers, P_{cs}. The shaded region represents the range of P_{cs} reported in the literature, summarized in table 5.

$$B_{j,t} = B_{j,0} \cdot \exp\left[\frac{Y_r}{B_j}(P_s - P_d) \cdot \Delta t\right] \tag{11}$$

where $B_{j,0}$ refers to the initial number of cells capable of catalyzing the jth reaction and Δt denotes the change in time. According to equation (11), when $P_d > P_s$, the population size decreases until power supply is equal to demand for maintenance. Under these conditions, equation (11) does not necessarily lose meaning, but the yield coefficient does. If the rate at which cells no longer became viable were known, which in principle is a function of environmental conditions, a decay constant could be substituted for Y_j in equation (11) to model the decrease in size of a microbial functional group. Equation (11) can be rearranged to calculate doubling/replacement times, $t_{d/r}$:

$$t_{d/r} = \frac{B_j \ln 2}{Y_j(P_s - P_d)}. \tag{12}$$

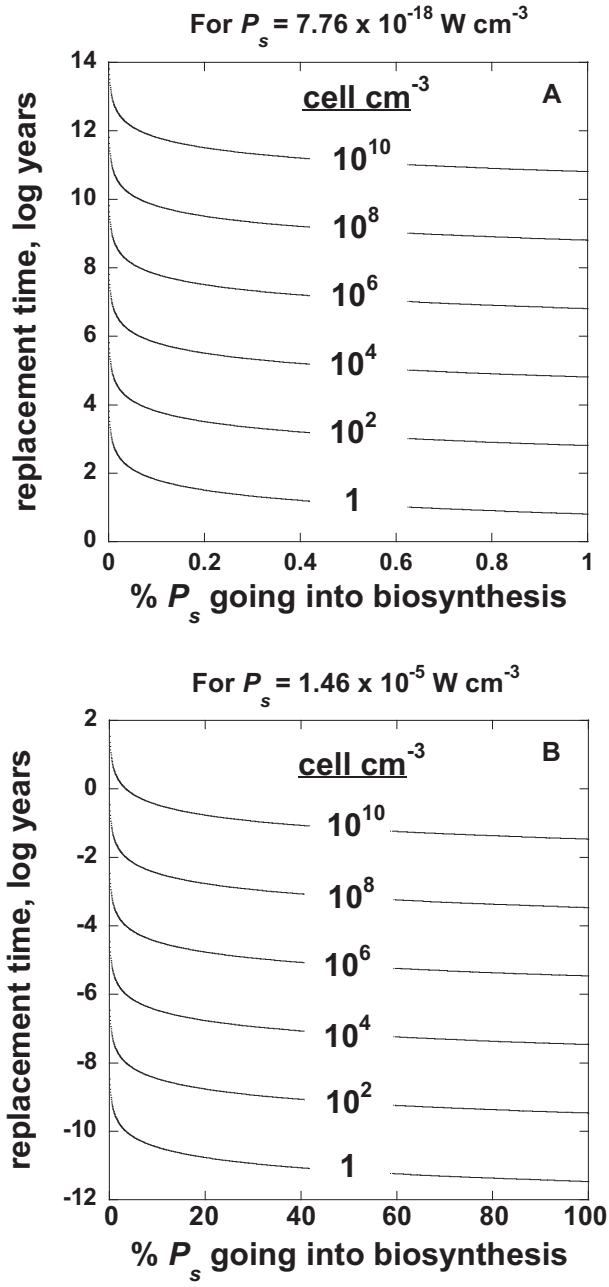

Fig. 4. Replacement or doubling times, $t_{r/d}$, for different numbers of microorganisms as a function of the percentage of catabolic power, P_s, that goes into biosynthesis for the (A) lowest and (B) highest values of P_s shown in figure 1 and table 2.

Values of doubling/replacement times for microbial populations of different sizes are shown in figure 4, calculated using the smallest (fig. 4A) and largest (fig. 4B) catabolic powers computed above, listed in table 2, equation (12) and $Y = 4.40 \times 10^8$ cells /J (in

table 7). These values of $t_{d/r}$ are shown as a function of the percentage of cataobolic power, P_s, that is converted into biosynthesis. A number of features of microbial activity can be seen in the panels depicted in figure 4. For both plots, the point at which the curves intersect the y-axis on the right hand side of the figures is the amount of time that it takes to double/replace a microbial population if 100 percent of the catabolic power is translated into biomass. Although this is impossible based on the 2nd law of thermodynamics alone, it does place a minimum limit on the replacement times for microbial populations of different sizes operating under a broad spectrum of (rate · energy) combinations. Another feature of these panels in figure 4 is that, for all of the population sizes considered, calculated replacement times increase slowly as the percentage of P_s that goes into biomass synthesis decreases from 100 to about 10 percent (the curves in fig. 4 are nearly flat over this range). As the amount of power going into biosynthesis falls below 10 percent of P_s, replacement times increase asymptotically towards infinity. That is, the replacement/doubling times for organisms that do not convert much catabolic power into biosynthesis take far longer to turnover their biomass than those that are able to harness a greater percentage of the available power supply. This is a quantitative statement showing that for two populations of microorganisms of the same size and living at the same power level, low-power adapted organisms (that is, those that use a greater proportion of their catabolic power to synthesize biomolecules) have faster doubling times than those less accustomed to low power. Note that though the plots in figure 4 appear to look the same, the y-axes cover very different scales.

Another utility of plots such as those shown in figure 4 is that the likely population size of active microorganisms can be constrained given catalytic rates and Gibbs energies of reactions. For example, for the high catabolic power considered in figure 4A, the replacement times of 10^8 cell cm^{-3} with 10 percent power going into biosynthesis is ~30 hours. For a population two orders of magnitude smaller, the replacement time would be half an hour. For even smaller populations, the turnover times for this power level become nonsensical. On the low-power end of the catabolic spectrum, it can be seen in figure 4B that large population sizes have replacement times that strain credulity. For instance, for a microbial population of 10^8 cells cm^{-3} realizing 7.76×10^{-18} W cm^{-3} and converting 1 percent of this into biomass would have a turnover time greater than the age of the universe.

The calculations underlying figure 4 can also shed light on the long replacement/doubling times of thousands of years that have recently been reported by Hoehler and Jørgensen (2013). If organisms in such circumstances are only maintaining molecular integrity by preventing the racemization of amino acids and the depurination of nucleic acids, something like a basal maintenance power, the power required to do this per cell would take on a much lower value than the values of P_{cs} reported in table 5. An alternative explanation for such long replacement times is that a smaller number of active microorganisms can account for the observed catabolic power being dissipated; thus, biomass replacement times would be on the order of months, not thousands of years. Whatever the interpretation, figure 4 quantitatively shows that microbial replacement/doubling time is a function of the percentage of catabolic power that is used to synthesize new biomass and the number of organisms that are active.

Constraining Catalysis Rates and Catabolic Power Used in the Deep Biosphere

The previous two sections detail how microbial activity levels and population sizes are quantitatively linked to power availability. In the following two sections, the equations summarized above are used to constrain likely catabolic rates in two well-characterized deep settings: marine sediments in the relatively high energy Peru Margin and low energy South Pacific Gyre. At both sites, the pore water chemistry and microbial cell counts are known as a function of depth. Furthermore, a recent study

computed the Gibbs energies of several plausible catabolic reactions at different depths in these sediments (LaRowe and Amend, 2014). These values of ΔG_r can be used in conjunction with the cell count data and yield coefficients listed in table 7 to estimate the rates of catalysis and the percentage of catabolic power conserved in the form of biomass in these environments.

Study site overview.—The Peru Margin (PM) site (IODP site 1229, 10°58.5721′S, 77°57.4590′W for hole 1229A), covered by ~150 m of water, underlies a zone of high primary productivity that has resulted in an average sedimentation rate of 24 m/MY (D'Hondt and others, 2003). As a result, the sediments here are rich in organic matter (1-12% TOC by weight) (Jørgensen and others, 2003) and EAs such as O_2 and NO_3^- disappear in the upper few centimeters of the sediment column. Sulfate pore water concentrations initially decreases as a function of depth, but then increase again owing to diffusion from a deep source. In particular, a Miocene brine supplies sulfate and other ions to the sediment column from below creating complex nutrient profiles. Although inner-shelf environments (water depth <150 m) only cover 5.8 percent of global ocean settings, a disproportionately large amount of primary production occurs there (Thullner and others, 2009). The concentration profiles of nitrate, sulfate, DIC, ammonium, sulfide, methane, Mn^{2+}, and Fe^{2+} are thought to be influenced by organic matter degradation (D'Hondt and others, 2004).

The slow sedimentation rate (1.1 m/M.Y.) and very deep water (5695 m) at the South Pacific Gyre (SPG) site (IODP site 1365, 23°51.0493′S, 165°38.6624′W for hole 1365A) are typical of open-ocean sites far from land (D'Hondt and others, 2011). Because open ocean sites comprise half or more of all ocean environments (Thullner and others, 2009), SPG sediments represent, by volume, a substantial portion of Earth's ecosystems. The low sedimentation rates and correspondingly tiny amounts of organic matter delivered to the ocean floor result in low biomass concentrations (D'Hondt and others, 2009). The near absence of electron donors at this site means that electron acceptors such as O_2 and NO_3^- can penetrate deep into the sediment column. D'Hondt and others (2009) suggest that oxygen and nitrate are the dominant EAs and that radiolytic hydrogen and organic matter are the most common EDs. However, the Gibbs energy calculations reported by LaRowe and Amend (2014) reveal that the oxidation of Fe^{2+} and Mn^{2+} both provide more energy than the oxidation of H_2 or organic matter throughout the sediment column.

Catabolic rates and power conserved as biomass.—The Gibbs energies of several plausible energy-providing reactions in PM and SPG sediments that were calculated in LaRowe and Amend (2014) are shown in figure 5 in units of kJ per mole of electron transferred, kJ $(\text{mol } e^-)^{-1}$. The prevailing temperature, pressure and composition of the pore fluids in these sediments were explicitly taken into account in these calculations. Note in figure 5 that the reactions separate into two groups for both sites. The high energy group of reactions, which typically yield between 70 to 105 kJ $(\text{mol } e^-)^{-1}$, rely on O_2, NO_3^- or MnO_2 as oxidants, while the low energy group of reactions, yielding 20 to 0 kJ $(\text{mol } e^-)^{-1}$, are methanogenesis and reactions with sulfate and FeOOH (goethite in this case) as electron acceptors. The most exergonic reactions are the aerobic oxidation of H_2 and organic matter, OM, in SPG sediments, but this site does not feature the fastest microbial metabolic rates or the largest biomass. Similarly, the lower energy yields in PM sediments do not result in commensurately lower microbial cell numbers (fig. 6). In fact, the cell counts in PM sediments are several orders of magnitude higher at all depths than those at SPG, the site of the most exergonic reactions considered. Either the rates of catalysis, and therefore the power of catabolism, P_s, must be far greater at PM than at SPG, or the percentage of catabolic power that is conserved as biomass at PM is far higher than at SPG. A number of scenarios are discussed below.

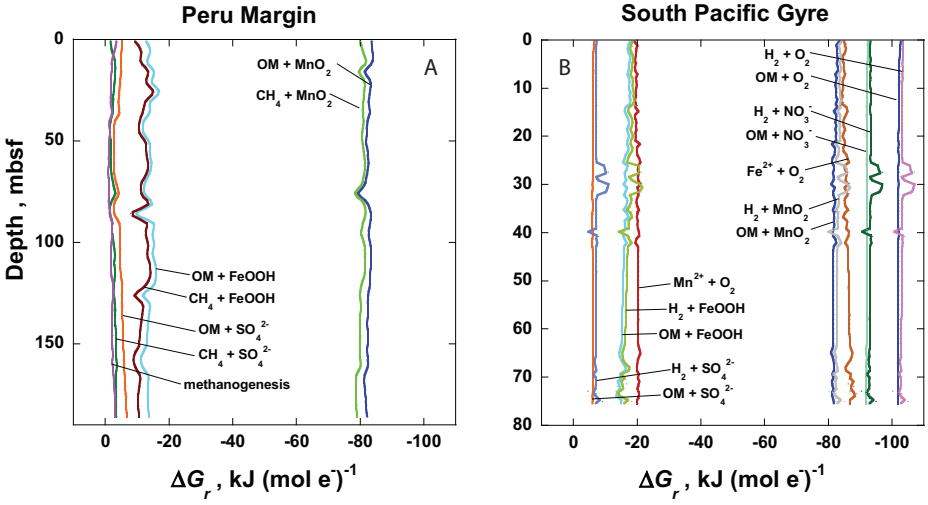

Fig. 5. Gibbs energies, ΔG_r, of several plausible reactions that microorganisms could be catalyzing in (A) Peru Margin and (B) South Pacific Gyre sediments as a function of depth. For each reaction, only the electron donor and acceptor are shown. After LaRowe and Amend (2014), which is where the full reactions can be found.

The knallgas reaction ($O_2 + H_2$) has been proposed as a catabolic pathway in SPG sediments (D'Hondt and others, 2009). By combining values of ΔG_r taken from LaRowe and Amend (2014), cell count data for SPG sediments, and a range of P_{cs} values for O_2 reduction (table 5), rates of O_2 reduction by H_2 in SPG sediments are calculated using a rearranged version of equation (3). The resulting range of reaction rates are shown in units of nmol cm^{-3} d^{-1} in figure 7 (the space between the solid lines). These rates are compared to those reported for O_2 reduction in North Pacific Gyre, NPG, sediments by (Røy and others, 2012) (shaded box). Although the NPG sediments sampled from site 11 on R/V Knorr voyage 195 are located thousands of kilometers from SPG sediments, these sites share many attributes. Both sites lie under 5.5 to 6 km of water, are far from land, receive little organic matter, have similar sediment thicknesses, sedimentation rates and O_2 profiles and oxygen penetrates to at least 30 m below the sediment water interface (D'Hondt and others, 2009; D'Hondt and others, 2011; Røy and others, 2012). Furthermore, Røy and others, 2012 have used the O_2 concentrations as a function of depth to model the rates of its consumption by microbial activity in NPG. However, there are not enough published geochemical data to carry out the type of Gibbs energy calculations that have been used to characterize SPG sediments. And although cell count data for NPG sites are available in graphical form for an undifferentiated collection of multiple NPG drill sites (Kallmeyer and others, 2012), cell counts at NPG site 11 as a function of depth, where the O_2 rate modeling has been carried out, are also not available. So, in a first approximation, the cell count data (D'Hondt and others, 2011) and Gibbs energy calculations that have been carried out describing SPG sediments (LaRowe and Amend, 2014) are combined with the O_2 consumption rates calculated for NPG sediments (Røy and others, 2012) in order to investigate how the equations presented above can be used to reveal the connections between microbial catabolic rates and energetics, maintenance power and populations sizes in ocean sediments that underlie low primary productivity regions of the ocean.

It can be seen in figure 7 that the range of O_2 reduction rates calculated in this study overlap with those determined by Røy and others (2012). However, the lowest

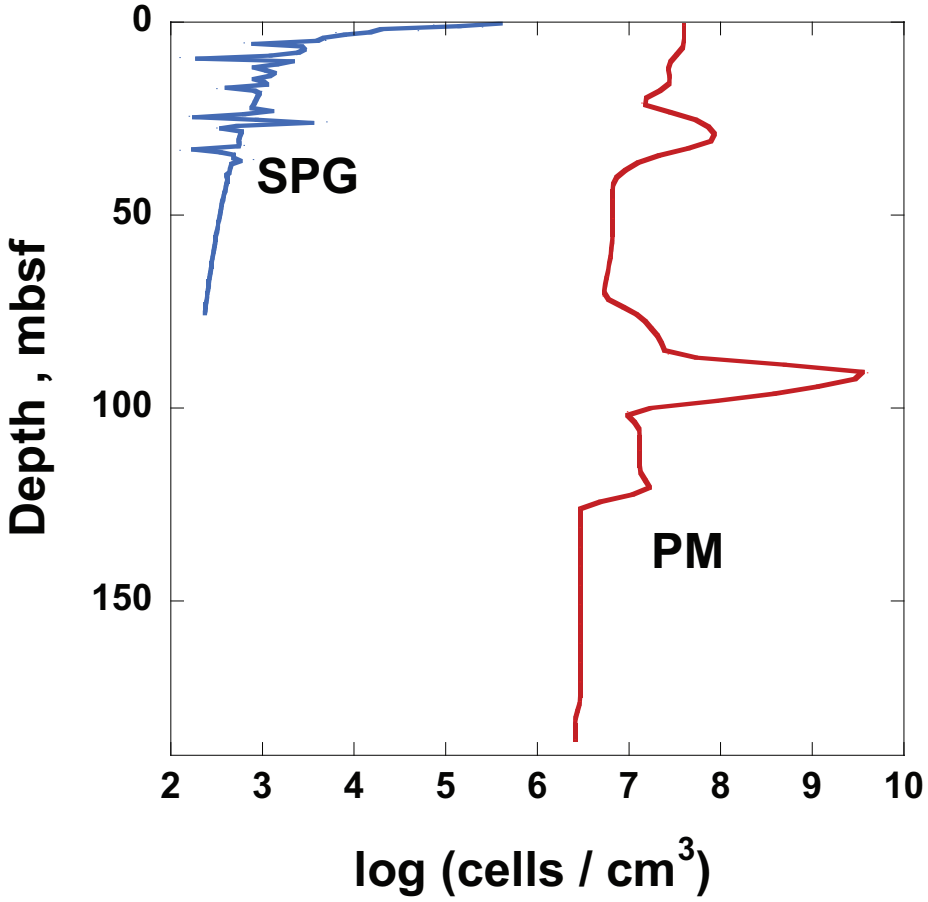

Fig. 6. Microbial cell counts in Peru Margin and South Pacific Gyre sediments. After LaRowe and Amend (2014). These values are interpolations of cell count data given by D'Hondt and others (2004) and D'Hondt and others (2009) respectively.

rates published by (Røy and others, 2012), 2.7×10^{-6} nmol O_2 cm^{-3} d^{-1} (left side of the shaded box), lie about 2 orders of magnitude lower than the lowest calculated in this study. One of the most straightforward explanations for this discrepancy is that the maintenance powers reported in the literature (table 5), which were determined for high-energy systems, are far higher than the cell-specific basal power demands of microorganisms in SPG sediments.

Rather than relying on values of cell-specific maintenance power reported in the literature, values of P_{cs} can be estimated by combining data sets: the rates of O_2 reduction reported by Røy and others (2012) and the cell count data from D'Hondt and others (2011). The resulting values of P_{cs} are shown in figure 8 (solid lines), where it can be seen that P_{cs} for microorganisms in very-low energy sediments slightly overlap with those that are summarized in table 5 for O_2 consumption (shaded area). However, the lowest computed values of P_{cs} (from the lowest rates reported in Røy and others, 2012) are several orders of magnitude lower than the values of P_{cs} in table 5. It should be noted that some of these computed values of P_{cs} are within the range of the lowest reported values of P_{cs} for any metabolism (dashed line in fig. 8). Still, the lowest

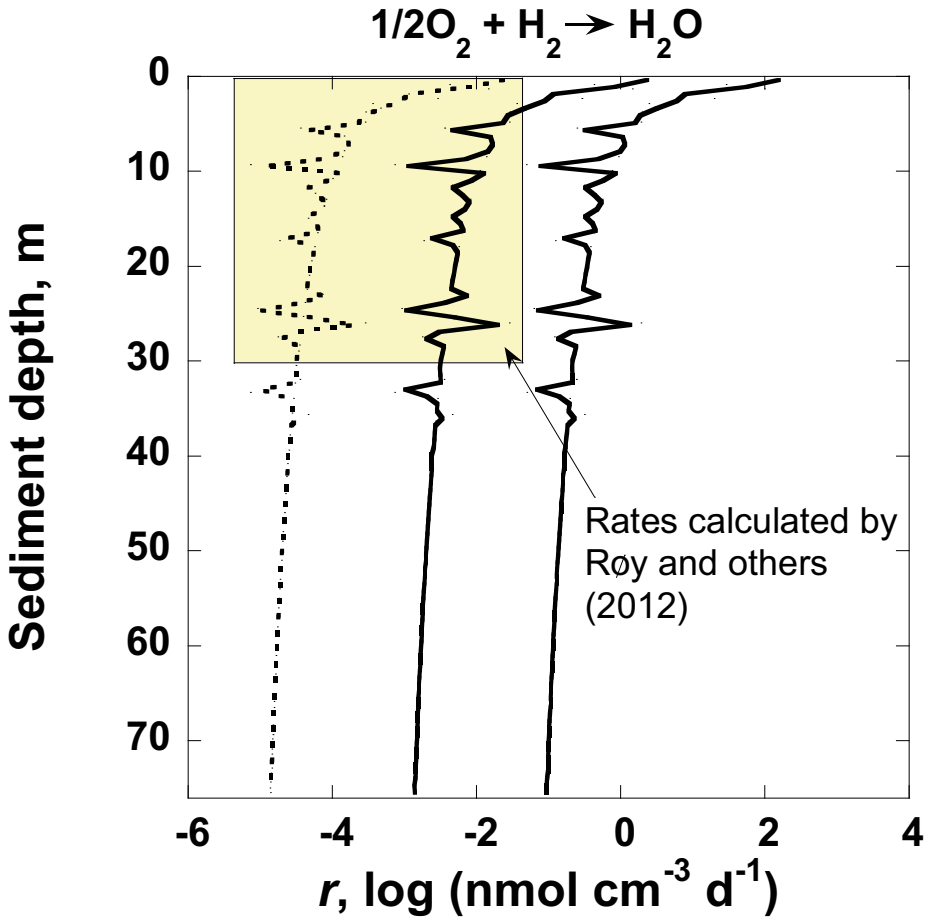

Fig. 7. Calculated catabolic reaction rates, r, for the knallgas reaction in South Pacific Gyre sediments for the lowest and highest values of single-cell maintenance power requirements, P_{cs}, reported in the literature for O_2 reduction (table 5)—solid lines. The dashed line refers to reaction rates for the knallgas reaction calculated assuming that only 1% of the cells counted in SPG sediments are actively catalyzed this reaction and using the lowest O_2 reduction value of P_{cs} from table 5. The shaded box indicates the range of O_2 reduction rates in North Pacific Gyre sediments reported by Røy and others (2012).

calculated values of P_{cs} are about two orders of magnitude less than the lowest that have been reported. Given the large range of P_{cs} values in table 5—the highest is nearly 250,000 times larger than the lowest—it could plausibly be the case that in very low energy environments such as SPG/NPG, the microorganisms can be characterized by values P_{cs} values 1 to 2 orders of magnitude lower than those in table 5. It should be noted that these calculations assume that all of the cells counted in SPG sediments are actively catalyzed in the knallgas reaction. If some of these cells are inactive or not able to catalyze in this reaction or were not counted properly, then the computed values of P_{cs} would fall closer to the values listed in table 5. The dashed line in figure 7 corresponds to an extreme scenario in which only 1 percent of the cells in these sediments are actively catalyzed in the knallgas reaction. In addition, the knallgas reaction may not represent the pathway of O_2 consumption and that Røy and others (2012) do not propose a particular ED being oxidized by O_2 in NPG sediments. In SPG

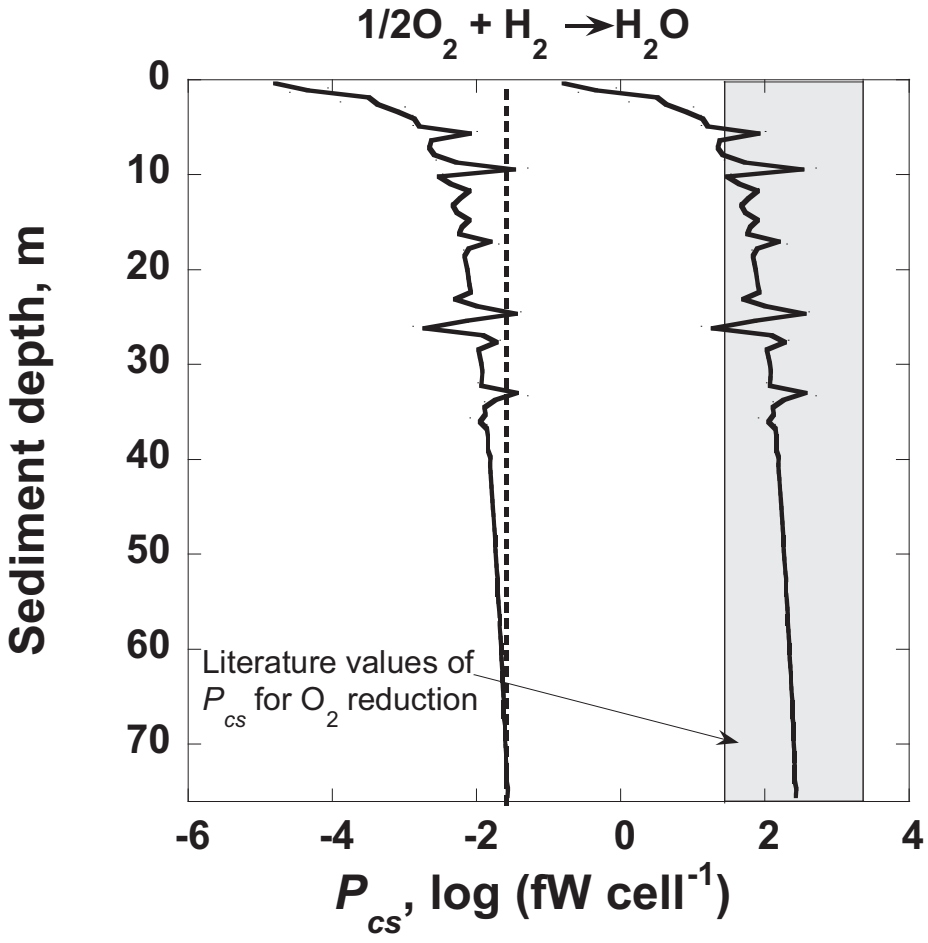

Fig. 8. Calculated values of single-cell maintenance power requirements, P_{cs}, for microorganisms catalyzing the knallgas reaction in South Pacific Gyre sediments using the maximum and minimum values of O_2 reduction rates reported in North Pacific Gyre sediments (Røy and others, 2012). The shaded box refers to the range of P_{cs} for O_2 reduction reported in the literature and the vertical dashed line designates the lowest reported value of P_{cs} for any type of metabolism (table 5).

sediments, for instance, it can be seen in figure 5B that organic matter, Fe^{2+} and Mn^{2+} are all plausible EDs, which might also be the case in NPG sediments. In fact, LaRowe and Amend (2014) show that Fe^{2+} and Mn^{2+} oxidation provide more energy per cm^3 of sediment that H_2 or organic matter at SPG, suggesting that these two reactions could be the dominant sinks of O_2.

In a similar set of calculations, rates of sulfate reduction coupled to organic matter degradation (OM + SO_4^{2-}) were computed in Peru Margin sediments. These calculations, shown in figure 9, were carried out using values of ΔG_r taken from LaRowe and Amend (2014), cell counts taken from D'Hondt and others (2003) and the minimum and maximum values of cell-specific maintenance powers for sulfate reduction shown in table 5. As with the results shown in figure 8, these are the rates of sulfate reduction required to maintain the biomass observed to exist in these sediments. It can be seen in figure 9 that whether the highest or lowest reported values of P_{cs} are used in the

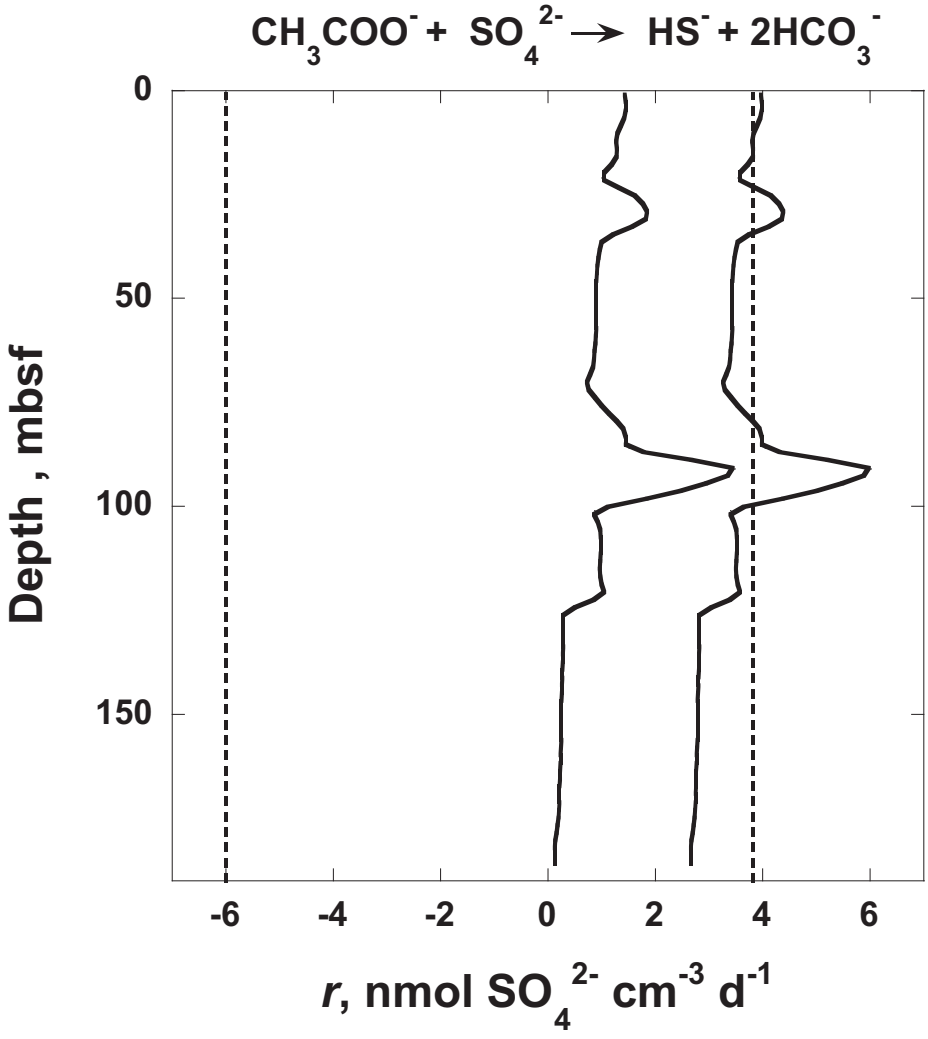

Fig. 9. Catabolic rate, *r*, of sulfate reduction coupled to organic matter (acetate) oxidation in Peru Margin sediments using the highest and lower values of single-cell maintenance power requirements, P_{cs}, reported in the literature for sulfate reduction, solid lines (table 5). The vertical dashed lines correspond to the highest of lowest rates of sulfate reduction arising from the highest and lowest values of P_{cs} reported in the literature for all metabolisms.

calculations, sulfate reduction rates in PM sediments vary by three orders of magnitude (solid lines). There is no simple relationship between depth and reaction rates since there are two sulfate-methane transition zones in these sediments (D'Hondt and others, 2004). For instance, the highest rates occur about 90 m into the sediment—not near the surface as with the SPG reaction rates. Also, the calculated sulfate reduction rates at a depth of 90 m exceed the highest values of sulfate reduction shown in table 2, which are mostly for settings near the SWI, for the scenario in which cell-specific power requirements are high. If, however, values of P_{cs} in PM sediments are more similar to the lower P_{cs} value, then the calculated rates of sulfate reduction fall within the range listed in table 2. As with SPG, values of P_{cs} in the deep biosphere could be lower than

those that have been observed so far (table 5). Yet, the calculations shown in figure 9 show that those reported can be used with equation (5) to predict reaction rates similar to those reported in the literature for sulfate reduction in other marine sediments even if maintenance power needs are a couple orders of magnitude lower than 0.32 fW $cell^{-1}$, the lowest reported value of P_{cs} for sulfate reducers.

The reaction rates for PM, which are >1 nmol SO_4^{2-} cm^{-3} d^{-1}, are significantly higher than the O_2 reduction rates reported for SPG/NPG. This makes sense given the several orders of magnitude difference in cell counts for these sites (fig. 6). As with SPG/NPG, other reactions could be supporting the microbial communities in these sediments (see fig. 5A)—the calculations represented in figure 9 are merely a demonstration of the utility of the approach summarized in this contribution. This would mean fewer sulfate reducers using organic matter, but the larger point here is that the physiological characteristics of microorganisms living in the deep biosphere can be teased out given cell counts and the geochemistry of their setting and the equations presented above.

CONCLUDING REMARKS

The equations and calculations summarized above establish a rigorously defined method for quantifying the activity level of microorganisms in any environment. Depending on the input data, several biogeochemical parameters can be constrained, including population sizes, basal power demands, catabolic rates, microbial growth rates and doubling/replacement times. This first-principles approach is especially useful for describing process rates in the deep biosphere since many of these environments are difficult to access and tend to be poorly characterized, at least from a biogeochemical perspective (Orcutt and others, 2014).

In summary, using data already available in the literature and calculated Gibbs energies, the range of catabolic power available in the marine subsurface from several metabolisms has been quantified (fig. 1). A simple relationship between catabolic power, maintenance power requirements and population sizes has been established (fig. 3). An energy-based model for calculating the biomass yield for a given amount of catabolic power has been developed that takes into account the prevailing environmental conditions. The replacement/doubling times for different microbial population sizes supplied by a range of catabolic power has been calculated and illustrated (fig. 4). Gibbs energies and cell count data for two marine deep sediment environments have been processed with the equations discussed above to reveal potential basal power requirements in an energy starved environment and/or the percentage of microorganisms that are active there (fig. 8). Furthermore, potential catabolic reaction rates have been estimated using the available geochemical data, Gibbs energy calculations, cell counts and values of maintenance power requirements (figs. 8 and 9). In the course of this study, catabolic reactions rates in the marine subsurface, maintenance power requirements and biomass yield coefficients were tabulated and summarized (tables 2, 5 and 6). Additionally, standard state values of the Gibbs energy of half-reactions describing the oxidation and reduction of a variety of electron donors and acceptors, respectively, have been tabulated as a function of temperature (table 3). The quantitative relationships developed above directly relate the geochemical parameters that describe environments to the size of microbial populations in them. For instance, when cell count data are available in conjunction with ΔG_r and reaction rates, then values of maintenance power requirements can be constrained. Similarly, literature values of cell-specific maintenance powers can be used to estimate reactions rates when values of ΔG_r and B_j are known.

ACKNOWLEDGMENTS

Financial assistance was provided by the Center for Dark Energy Biosphere Investigations (C-DEBI) and the NASA Astrobiology Institute—Life Underground (NAI-LU, Award#NNA13AA92A). This is C-DEBI contribution 234 and NAI-LU contribution 005. Thorough reviews from Bo Barker Jørgensen, Andreas Teske and an anonymous review have significantly improved this contribution.

Appendix: Thermodynamic Calculations

In this study, values of ΔG_r are calculated using

$$\Delta G_r = -RT \ln \frac{K_r}{Q_r}, \tag{A-1}$$

where K_r and Q_r refer to the equilibrium constant and reaction quotient of the reaction, respectively, R represents the gas constant, and T denotes temperature in Kelvin. Values of K_r were calculated using the revised-HKF equations of state (Helgeson and others, 1981; Shock and others, 1992; Tanger and Helgeson, 1988), the SUPCRT92 software package (Johnson and others, 1992), and thermodynamic data taken from a number of sources (Shock and Helgeson, 1988; Shock and others, 1989; Shock and Helgeson, 1990; Sverjensky and others, 1997; Schulte and others, 2001; Dick and others, 2006; LaRowe and Helgeson, 2006).

Values of Q_r were calculated using

$$Q_r = \prod_i a_i^{\nu_i}, \tag{A-2}$$

where a_i stands for the activity of the ith species and ν_i corresponds to the stoichiometric coefficient of the ith species in the reaction of interest. Values of a_i are related to the concentration of the ith species, C_i, through

$$a_i = \gamma_i \left(\frac{C_i}{C_i^0} \right) \tag{A-3}$$

where γ_i stands for the activity coefficient of the ith species and C_i^0 refers to the concentration of the ith species under standard state conditions, which is taken to be equal to one molal referenced to infinite dilution. Values of γ_i were in turn computed as a function of temperature and ionic strength using an extended version of the Debye-Hückel equation (Helgeson, 1969).

REFERENCES

Amend, J. P., and Shock, E. L., 1998, Energetics of amino acid synthesis in hydrothermal ecosystems: Science, v. 281, n. 5383, p. 1659–1662, http://dx.doi.org/10.1126/science.281.5383.1659

Amend, J. P., McCollom, T. M., Hentscher, M., and Bach, W., 2011, Catabolic and anabolic energy for chemolithoautotrophs in deep-sea hydrothermal systems hosted in different rock types: Geochimica et Cosmochimica Acta, v. 75, n. 19, p. 5736–5748, http://dx.doi.org/10.1016/j.gca.2011.07.041

Amend, J. P., LaRowe, D. E., McCollom, T. M., and Shock, E. L., 2013, The energetics of organic synthesis inside and outside the cell: Philosophical Transactions of the Royal Society B, v. 368, n. 1622, p. 1–15, http://dx.doi.org/10.1098/rstb.2012.0255

Amy, P. S., and Haldeman, D. L., 1997, The Microbiology of the Terrestrial Deep Subsurface: Boca Raton, USA, CRC Lewis Publishers, p. 356.

Arndt, S., Brumsack, H.-J., and Wirtz, K. W., 2006, Cretaceous black shales as active bioreactors: A biogeochemical model for the deep biosphere encountered during ODP Leg 207 (Demerara Rise): Geochimica et Cosmochimica Acta, v. 70, n. 2, p. 408–425, http://dx.doi.org/10.1016/j.gca.2005.09.010

Bach, W., and Edwards, K. J., 2003, Iron and sulfide oxidation within the basaltic ocean crust: Implications for chemolithoautotrophic microbial biomass production: Geochimica et Cosmochimica Acta, v. 67, n. 20, p. 3871–3887, http://dx.doi.org/10.1016/S0016-7037(03)00304-1

Battley, E. H., 1991, An alternative method of calculating the heat of growth of *Escherichia coli* K-12 on succinic acid: Biotechnology and Bioengineering, v. 38, n. 5, p. 480–492, http://dx.doi.org/10.1002/bit.260380506

Beyeler, W., Rogers, P. L., and Fiechter, A., 1984, A simple technique for the direct determination of maintenance energy coefficient: An example with *Zymomonas mobilis*: Applied Microbiology and Biotechnology, v. 19, n. 4, p. 277–280, http://dx.doi.org/10.1007/BF00251851

Biddle, J. F., Lipp, J. S., Lever, M. A., Lloyd, K. G., Sørensen, K. B., Anderson, R., Fredricks, H. F., Elvert, M., Kelly, T. J., Schrag, D. P., Sogin, M. L., Brenchley, J. E., Teske, A., House, C. H., and Hinrichs, K.-U., 2006, Heterotrophic Archaea dominate sedimentary subsurface ecosystems off Peru: Proceedings of the National Academy of Sciences, v. 103, n. 10, p. 3846–3851, http://dx.doi.org/10.1073/pnas.0600035103

Blackburne, R., Vadivelu, V. M., Yuan, Z., and Keller, J., 2007, Kinetic description of an enriched *Nitrospira* culture with comparison to *Nitrobacter*: Water Research, v. 41, n. 14, p. 3033–3042, http://dx.doi.org/10.1016/j.watres.2007.01.043

Boettger, J., Lin, H.-T., Cowen, J. P., Hentscher, M., and Amend, J. P., 2013, Energy yields from chemolithotrophic metabolisms in igneous basement of the Juan de Fuca ridge flank system: Chemical Geology, v. 337–338, p. 11–19, http://dx.doi.org/10.1016/j.chemgeo.2012.10.053

Chapelle, F. H., and Lovley, D. R., 1990, Rates of microbial metabolism in deep coastal-plain aquifers: Applied and Environmental Microbiology, v. 56, n. 6, p. 1865–1874.

Chesbro, W., Evans, T., and Eifert, R., 1979, Very slow growth of *Escherichia coli*: Journal of Bacteriology, v. 139, n. 2, p. 625–638.

Colwell, F. S., and D'Hondt, S., 2013, Nature and extent of the deep biosphere: Reviews in Mineralogy and Geochemistry, v. 75, p. 547–574, http://dx.doi.org/10.2138/rmg.2013.75.17

Cowen, J. P., 2004, The microbial biosphere of sediment-buried oceanic basement: Research in Microbiology, v. 155, n. 7, p. 497–506, http://dx.doi.org/10.1016/j.resmic.2004.03.008

Dale, A. W., Sommer, S., Haeckel, M., Wallmann, K., Linke, P., Wegener, G., and Pfannkuche, O., 2010, Pathways and regulation of carbon, sulfur and energy trasnfer in marine sediments overlying methane gas hydrates on the Opouawe Bank (New Zealand): Geochimica et Cosmochimica Acta, v. 74, n. 20, p. 5763–5784, http://dx.doi.org/10.1016/j.gca.2010.06.038

Daniels, L., Sparling, R., and Sprott, G. D., 1984, The bioenergetics of methanogenesis: Biochimica et Biophysica Acta, v. 768, n. 2, p. 113–163, http://dx.doi.org/10.1016/0304-4173(84)90002-8

de Angelis, M. A., Lilley, M. D., Olson, E. J., and Baross, J. A., 1993, Methane oxidation in deep-sea hydrothermal plumes of the Endeavor Segment of the Juan de Fuca Ridge: Deep-Sea Research I: Oceanographic Research papers, v. 40, n. 6, p. 1169–1186, http://dx.doi.org/10.1016/0967-0637(93)90132-M

de Poorter, L. M. I., Geerts, W. J., and Keltjens, J. T., 2007, Coupling of *Methanothermobacter thermoautotrophicus* methane formation and growth in fed-batch and continuous cultures under different H_2 gassing regimes: Applied and Environmental Microbiology, v. 73, n. 3, p. 740–749, http://dx.doi.org/10.1128/AEM.01885-06

D'Hondt, S., Rutherford, S., and Spivack, A. J., 2002, Metabolic activity of subsurface life in deep-dea sediments: Science, v. 295, n. 5562, p. 2067–2070, http://dx.doi.org/10.1126/science.1064878

D'Hondt, S., Jorgensen, B. B., Miller, D. J., and others, 2003, Leg 201 Summary: Proceedings of the Integrated Ocean Drilling Program, v. 201, p. 1–81, http://dx.doi.org/10.2973/odp.proc.ir.201.101.2003

D'Hondt, S., Jørgensen, B. B., Miller, D. J., Batzke, A., Blake, R., Cragg, B. A., Cypionka, H., Dickens, G. R., Ferdelman, T., Hinrichs, K. U., Holm, N. G., Mitterer, R., Spivack, A., Wang, G. Z., Bekins, B., Engelen, B., Ford, K., Gettemy, G., Rutherford, S. D., Sass, H., Skilbeck, C. G., Aiello, I. W., Guerin, G., House, C. H., Inagaki, F., Meister, P., Naehr, T., Niitsuma, S., Parkes, R. J., Schippers, A., Smith, D. C., Teske, A., Wiegel, J., Padilla, C. N., and Acosta, J. L. S., 2004, Distributions of microbial activities in deep subseafloor sediments: Science, v. 306, n. 5705, p. 2216–2221, http://dx.doi.org/10.1126/science.1101155

D'Hondt, S., Spivack, A. J., Pockalny, R., Ferdelman, T. G., Fischer, J. P., Kallmeyer, J., Abrams, L. J., Smith, D. C., Graham, D., Hasiuk, F., Schrum, H., and Stancin, A. M., 2009, Subseafloor sedimentary life in the South Pacific Gyre: Proceedings of the National Academy of Sciences, v. 106, n. 28, p. 11651–11656, http://dx.doi.org/10.1073/pnas.0811793106

D'Hondt, S., Inagaki, F., Alvarez Zarikian, C. A., and the Expedition Scientists, 2011, Site U1365: Proceedings of the Integrated Ocean Drilling Program, v. 329.

Dick, J. M., LaRowe, D. E., and Helgeson, H. C., 2006, Temperature, pressure and electrochemical constraints on protein speciation: Group additivity calculation of the standard molal thermodynamic properties of ionized unfolded proteins: Biogeosciences, v. 3, p. 311–336, http://dx.doi.org/10.5194/bg-3-311-2006

Edwards, K. J., Bach, W., and McCollom, T. M., 2005, Geomicrobiology in oceanography: microbe–mineral interactions at and below the seafloor: TRENDS in Microbioliology, v. 13, n. 9, p. 449–456, http://dx.doi.org/10.1016/j.tim.2005.07.005

Edwards, K. J., Becker, K., and Colwell, F., 2012, The deep, dark energy biosphere: Intraterrestrial life on Earth: Annual Reviews in Earth Planetary Sciences, v. 40, p. 551–568, http://dx.doi.org/10.1146/annurev-earth-042711-105500

Fredickson, J. K., and Fletcher, M., 2001, Subsurface Microbiology and Biogeochemistry: New York, Wiley & Sons, p. 341.

Fredickson, J. K., and Onstott, T. C., 2001, Biogeochemical and geological significance of subsurface microbiology, *in* Fredickson, J. K., and Fletcher, M., editors, Subsurface Microbiology and Biogeochemistry: New York, John Wiley & Sons, p. 3–37.

Fredickson, J. K., Garland, T. R., Hicks, R. J., Thomas, J. M., Li, S. W., and McFadden, K. M., 1989, Lithotrophic and heterotrophic bacteria in deep subsurface sediments and their relation to sediment properties: Geomicrobiology Journal, v. 7, n. 1–2, p. 53–66, http://dx.doi.org/10.1080/01490458909377849

Galchenkov, V. F., Ivanov, M. V., and Lein, A. Y., 1989, Microbiological and biogeochemical processes in oceanic water as indicators of activity of submarine hydrotherms: Geokhimiya, p. 1075–1088.

Goma, G., Moletta, R., and Novak, M., 1979, Comments on the "Maintenance coefficient" changes during alcohol fermentation: Biotechnology Letters, v. 1, n. 1, p. 415–420, http://dx.doi.org/10.1007/BF01388078

Guerrero, R., 1998, Crucial crises in biology: life in the deep biosphere: International Microbiology, v. 1, p. 285–294.

Gupta, S. K., and Sharma, R., 1996, Biological oxidation of high strength nitrogenous wastewater: Water Research, v. 30, n. 3, p. 593–600, http://dx.doi.org/10.1016/0043-1354(95)00172-7

Heijnen, J. J., and van Dijken, J. P., 1992, In search of a thermodynamic description of biomass yields for the chemotrophic growth of microorganisms: Biotechnology and Bioengineering, v. 39, n. 8, p. 833–858, http://dx.doi.org/10.1002/bit.260390806

Helgeson, H. C., 1969, Thermodynamics of hydrothermal systems at elevated temperatures and pressures: American Journal of Science, v. 267, n. 7, p. 729–804, http://dx.doi.org/10.2475/ajs.267.7.729

Helgeson, H. C., Kirkham, D. H., and Flowers, G. C., 1981, Theoretical prediction of thermodynamic behavior of aqueous electrolytes at high pressures and temperatures: IV. Calculation of activity coefficients, osmotic coefficients, and apparent molal and standard and relative partial molal properties to 600 °C and 5 kb: American Journal of Science, v. 281, n. 10, p. 1249–1516, http://dx.doi.org/10.2475/ajs.281.10.1249

Helgeson, H. C., Richard, L., McKenzie, W. F., Norton, D. L., and Schmitt, A., 2009, A chemical and thermodynamic model of oil generation in hydrocarbon source rocks: Geochimica et Cosmochimica Acta, v. 73, p. 594–695, n. 3, http://dx.doi.org/10.1016/j.gca.2008.03.004

Hoehler, T. M., and Jørgensen, B. B., 2013, Micorbial life under extreme energy limitation: Nature Reviews Microbiology, v. 11, p. 83–94, http://dx.doi.org/10.1038/nrmicro2939

Holmkvist, L., Ferdelman, T. G., and Jørgensen, B. B., 2011, A cryptic sulfur cycle driven by iron in the methane zone of marine sediment (Aarhus Bay, Denmark): Geochimica et Cosmochimica Acta, v. 75, n. 12, p. 3581–3599, http://dx.doi.org/10.1016/j.gca.2011.03.033

Jetten, M. S. M., Stams, A. J. M., and Zehnder, A. J. B., 1992, Methanogenesis from acetate: a comparison of the acetate metabolism in *Methanothrix soehngenii* and *Methanosarcina* spp.: FEMS Microbiology Letters, v. 88, n. 3–4, p. 181–198, http://dx.doi.org/10.1111/j.1574-6968.1992.tb04987.x

Johnson, J. W., Oelkers, E. H., and Helgeson, H. C., 1992, SUPCRT92 - A software package for calculating the standard molal thermodynamic properties of minerals, gases, aqueous species, and reactions from 1 bar to 5000 bar and 0 °C to 1000 °C: Computers and Geosciences, v. 18, n. 7, p. 899–947, http://dx.doi.org/10.1016/0098-3004(92)90029-Q

Johnston, C. G., and Vestal, J. R., 1991, Photosynthetic carbon incorporation and turnover in Antarctic cryptoendolithic microbial communities: Are they the slowest-growing communities on Earth?: Applied and Environmental Microbiology, v. 57, n. 8, p. 2308–2311.

Jørgensen, B. B., 2011, Deep subseafloor microbial cells on physiological standby: Proceedings of the National Academy of Sciences of the United States of America, v. 108, n. 45, p. 18193–18194, http://dx.doi.org/10.1073/pnas.1115421108

——— 2012, Shrinking majority of the deep biosphere: Proceedings of the National Academy of Sciences of the United States of America, v. 109, n. 40, p. 15976–15977, http://dx.doi.org/10.1073/pnas.1213639109

Jørgensen, B. B., and Boetius, A., 2007, Feast and famine—microbial life in the deep-sea bed: Nature Reviews Microbiology, v. 5, p. 770–781, http://dx.doi.org/10.1038/nrmicro1745

Jørgensen, B. B., and D'Hondt, S., 2006, A starving majority deep beneath the seafloor: Science, v. 314, n. 5801, p. 932–934, http://dx.doi.org/10.1126/science.1133796

Jørgensen, B. B., D'Hondt, S. L., and Miller, D. J., 2003, Leg 201 Synthesis: Controls on micorbial communities in deeply buried sediments: Proceedings of the Ocean Drilling Program, Scientific Results, v. 201, p. 45, http://dx.doi.org/10.2973/odp.proc.sr.201.101.2006

Joye, S. B., Boetius, A., Orcutt, B. N., Montoya, J. P., Schulz, H. N., Erickson, M. J., and Lugo, S. K., 2004, The anaerobic oxidation of methane and sulfate reduction in sediments from Gulf of Mexico cold seeps: Chemical Geology, v. 205, n. 3–4, p. 219–238, http://dx.doi.org/10.1016/j.chemgeo.2003.12.019

Joye, S. B., Samarkin, V. A., Orcutt, B. N., MacDonald, I. R., Hinrichs, K.-U., Elvert, M., Teske, A. P., Lloyd, K. G., Lever, M. A., Montoya, J. P., and Meile, C. D., 2009, Metabolic variability in seafloor brines revealed by carbon and sulphur dynamics: Nature Geoscience, v. 2, p. 349–354, http://dx.doi.org/10.1038/ngeo475

Kallmeyer, J., and Boetius, A., 2004, Effects of temperature and pressure on sulfate reduction and anaerobic oxidation of methane in hydrothermal sediments of Guaymas Basin: Applied and Environmental Microbiology, v. 70, n. 2, p. 1231–1233, http://dx.doi.org/10.1128/AEM.70.2.1231-1233.2004

Kallmeyer, J., Pockalny, R., Adhikari, R. R., Smith, D. C., and D'Hondt, S., 2012, Global distribution of microbial abundance and biomass in subseafloor sediment: Proceedings of the National Academy of Sciences of the United States of America, v. 109, n. 40, p. 16213–16216, http://dx.doi.org/10.1073/pnas.1203849109

Kieft, T. L., and Phelps, T. J., 1997, Life in the slow lane: Activities of microorganisms in the subsurface, *in* Amy, P. S., and Haldeman, D. L., editors, The Microbiology of the Terrestrial Deep Subsurface: Boca Raton, USA, CRC Lewis, p. 137–163.

Kirchman, D. L., and Hanson, T. E., 2013, Bioenergetics of photoheterotrophic bacteria in the oceans: Environmental Microbiology Reports, v. 5, n. 2, p. 188–199, http://dx.doi.org/10.1111/j.1758-2229.2012.00367.x

Konopka, A., 2000, Microbial physiological state at low growth rate in natural and engineered ecosystems: Current Opinion in Microbiology, v. 3, n. 3, p. 244–247, http://dx.doi.org/10.1016/S1369-5274(00)00083-7

LaRowe, D. E., and Amend, J. P., 2014, Energetic constraints on life in marine deep sediments, *in* Kallmeyer, J., and Wagner, K., editors, Life in Extreme Environments: Microbial Life in the Deep Biosphere: Berlin, de Gruyter, p. 279–302.

LaRowe, D. E., and Dick, J. M., 2012, Calculation of the standard molal thermodynamic properties of crystalline peptides: Geochimica et Cosmochimica Acta, v. 80, p. 70–91, http://dx.doi.org/10.1016/j.gca.2011.11.041

LaRowe, D. E., and Helgeson, H. C., 2006, Biomolecules in hydrothermal systems: Calculation of the

standard molal thermodynamic properties of nucleic-acid bases, nucleosides, and nucleotides at elevated temperatures and pressures: Geochimica et Cosmochimica Acta, v. 70, n. 18, p. 4680–4724, http://dx.doi.org/10.1016/j.gca.2006.04.010

LaRowe, D. E., and Regnier, P., 2008, Thermodynamic potential for the abiotic synthesis of adenine, cytosine, guanine, thymine, uracil, ribose and deoxyribose in hydrothermal systems: Origins of Life and of Biospheres, v. 38, n. 5, p. 383–397, http://dx.doi.org/10.1007/s11084-008-9137-2

LaRowe, D. E., Dale, A. W., and Regnier, P., 2008, A thermodynamic analysis of the anaerobic oxidation of methane in marine sediments: Geobiology, v. 6, n. 5, p. 436–449, http://dx.doi.org/10.1111/j.1472-4669.2008.00170.x

LaRowe, D. E., Dale, A. W., Amend, J. P., and Van Cappellen, P., 2012, Thermodynamic limitations on microbially catalyzed reaction rates: Geochimica et Cosmochimica Acta, v. 90, p. 96–109, http://dx.doi.org/10.1016/j.gca.2012.05.011

LaRowe, D. E., Dale, A. W., Aguilera, D. R., L'Heureux, I., Amend, J. P., and Regnier, P., 2014, Modeling micorbial reaction rates in a submarine hydrothermal vent chimney wall: Geochimica et Cosmochimica Acta, v. 124, p. 72–97, http://dx.doi.org/10.1016/j.gca.2013.09.005

Lein, A. Y., Pimenov, N. V., and Ivanov, M. V., 1997, Bacterial chemosynthesis and methanotrophy in the Manus and Lau basins ecosystems: Marine Geology, v. 142, p. 47–56, http://dx.doi.org/10.1016/S0025-3227(97)00040-6

Lennon, J. T., and Jones, S. E., 2011, Micorbial seed banks: the ecological and evolutionary implication of dormancy: Nature Reviews Microbiology, v. 9, p. 119–130, http://dx.doi.org/10.1038/nrmicro2504

Liu, J.-S., Vojinović, V., Patiño, R., Maskow, T., and von Stockar, U., 2007, A comparison of various Gibbs energy dissipation correlations for predicting micorbial growth yields: Thermochimica Acta, v. 458, n. 1–2, p. 38–46, http://dx.doi.org/10.1016/j.tca.2007.01.016

Lomstein, B. A., Langerhuus, A. T., D'Hondt, S., Jørgensen, B. B., and Spivack, A. J., 2012, Endospore abundance, micorbial growth and necromass turnover in deep sub-seafloor sediment: Nature, v. 484, p. 101–104, http://dx.doi.org/10.1038/nature10905

Lovley, D. R., and Chapelle, F. H., 1995, Deep subsurface microbial processes: Reviews of Geophysics, v. 33, n. 3, p. 365–381, http://dx.doi.org/10.1029/95RG01305

Maignien, L., Parkes, R. J., Cragg, B., Niemann, H., Knittel, K., Coulon, S., Akhmetzhanov, A., and Boon, N., 2013, Anaeorbic oxidation of methane in hypersaline cold seep sediments: FEMS Microbiology Ecology, v. 83, n. 1, p. 214–231, http://dx.doi.org/10.1111/j.1574-6941.2012.01466.x

Marschall, E., Jogler, M., Henssge, U., and Overmann, J., 2010, Large-scale distribution and activity patterns of an extremely low-light-adapted population of green sulfur bacteria in the Black Sea: Environmental Microbiology, v. 12, n. 5, p. 1348–1362, http://dx.doi.org/10.1111/j.1462-2920.2010.02178.x

McCollom, T. M., 2000, Geochemical constraints on primary productivity in submarine hydrothermal vent plumes: Deep-Sea Research Part I: Oceanographic Research Papers, v. 47, n. 1, p. 85–101, http://dx.doi.org/10.1016/S0967-0637(99)00048-5

——— 2007, Geochemical constraints on sources of metabolic energy for chemolithoautotrophy in ultramafic-hosted deep-sea hydrothermal systems: Astrobiology, v. 7, n. 6, p. 933–950, http://dx.doi.org/10.1089/ast.2006.0119

McCollom, T. M., and Amend, J. P., 2005, A thermodynamic assessment of energy requirements for biomass synthesis by chemolithoautotrophic micro-organisms in oxic and anoxic environments: Geobiology, v. 3, n. 2, p. 135–144, http://dx.doi.org/10.1111/j.1472-4669.2005.00045.x

McCollom, T. M., and Shock, E. L., 1997, Geochemical constraints on chemolithoautotrophic metabolism by microorganisms in seafloor hydrothermal systems: Geochimica et Cosmochimica Acta, v. 61, n. 20, p. 4375–4391, http://dx.doi.org/10.1016/S0016-7037(97)00241-X

McMahon, S., and Parnell, J., 2014, Weighing the deep continental biosphere: FEMS Microbiology Ecology, v. 87, n. 1, p. 113–120, http://dx.doi.org/10.1111/1574-6941.12196

Morono, Y., Terada, T., Nishizawa, M., Ito, M., Hillion, F., Takahata, N., Sano, Y., and Inagaki, F., 2011, Carbon and nitrogen assimilation in deep subseafloor micorbial cells: Proceedings of the National Academy of Sciences of the United States of America, v. 108, n. 45, p. 18295–18300, http://dx.doi.org/10.1073/pnas.1107763108

Nauhaus, K., Albrecht, M., Elvert, M., Boetius, A., and Widdel, F., 2007, *In vitro* cell growth of marine archaeal-bacterial consortia during anaerobic oxidation of methane with sulfate: Environmental Microbiology, v. 9, n. 1, p. 187–196, http://dx.doi.org/10.1111/j.1462-2920.2006.01127.x

Neijssel, O. M., and Tempest, D. W., 1976, Bioenergetic aspects of aerobic growth of *Klebsiella aerogens* NCTC 418 in Carbon-Limited and Carbon-Sufficient chemostat culture: Archives of Microbiology, v. 107, n. 2, p. 215–221, http://dx.doi.org/10.1007/BF00446843

Niemann, H., Duarte, J., Hensen, C., Omoregie, E., Magalhães, V. H., Elvert, M., Pinheiro, L. M., Kopf, A., and Boetius, A., 2006, Microbial methane turnover at mud volcanoes of the Gulf of Cadiz: Geochimica et Cosmochimica Acta, v. 70, n. 21, p. 5336–5355, http://dx.doi.org/10.1016/j.gca.2006.08.010

Okabe, S., Nielsen, P. H., and Characklis, W. G., 1992, Factors affecting micorbial sulfate reduction by *Desulfovibrio desulfuricans* in continuous culture: limiting nutrients and sulfide concentration: Biotechnology and Bioengineering, v. 40, n. 6, p. 725–734, http://dx.doi.org/10.1002/bit.260400612

Omoregie, E. O., Niemann, H., Mastalerz, V., de Lange, G. J., Stadnitskaia, A., Mascle, J., Foucher, J.-P., and Boetius, A., 2009, Microbial methane oxidation and sulfate reduction at cold seeps of the deep Eastern Mediterranean Sea: Marine Geology, v. 261, n. 1–4, p. 114–127, http://dx.doi.org/10.1016/j.margeo.2009.02.001

Orcutt, B., Boetius, A., Elvert, M., Samarkin, V., and Joye, S. B., 2005, Molecular biogeochemistry of sulfate reduction, methanogenesis and the anaerobic oxidation of methane at Gulf of Mexico cold seeps: Geochimica et Cosmochimica Acta, v. 69, n. 17, p. 4267–4281, http://dx.doi.org/10.1016/j.gca.2005.04.012

Orcutt, B. N., Sylvan, J. B., Knab, N. J., and Edwards, K. J., 2011, Microbial ecology of the dark ocean above, at, and below the seafloor: Microbiology and Molecular Biology Reviews, v. 75, n. 2, p. 361–422, http://dx.doi.org/10.1128/MMBR.00039-10

Orcutt, B. N., LaRowe, D. E., Biddle, J. F., Cowell, F. S., Glazer, B. T., Reese, B. K., Kirkpatrick, J. B., Lapham, L., Mills, H. J., Sylvan, J. B., Wankel, S. D., and Wheat, C. G., 2013, Microbial activity in the marine deep biosphere: Progress and prospects: Frontiers in Microbiology, v. 4, article 189, http://dx.doi.org/10.3389/fmicb.2013.00189

Orcutt, B. N., LaRowe, D. E., Lloyd, K. G., Mills, H., Orsi, W., Reese, B. K., Sauvage, J., Huber, J. A., and Amend, J. P., 2014, IODP deep biosphere research workshop report - A synthesis of recent investigations and discussion of new research questions and drilling targets: Scientific Drilling, v. 17, p. 61–66, http://dx.doi.org/10.5194/sd-17-61-2014

Parkes, R. J., Cragg, B. A., Fry, J. C., Herbert, R. A., Wimpenny, J. W. T., Allen, J. A., and Whitfield, M., 1990, Bacterial biomass and activity in deep sediment layers from the Peru Margin [and Discussion]: Philosophical Transactions of the Royal Society London A, v. 331, n. 1616, p. 139–153, http://dx.doi.org/10.1098/rsta.1990.0061

Parkes, R. J., Cragg, B. A., Bale, S. J., Getliff, J. M., Goodman, K., Rochelle, P. A., Fry, J. C., Weightman, A. J., and Harvey, S. M., 1994, Deep bacterial biosphere in Pacific Ocean sediments: Nature, v. 371, p. 410–413, http://dx.doi.org/10.1038/371410a0

Parkes, R. J., Cragg, B. A., and Wellsbury, P., 2000, Recent studies on bacterial populations and processes in subseafloor sediments: A review: Hydrogeology Journal, v. 8, n. 1, p. 11–28, http://dx.doi.org/10.1007/PL00010971

Parkes, R. J., Webster, G., Cragg, B. A., Weightman, A. J., Newberry, C. J., Ferdelman, T. G., Kallmeyer, J., Jørgensen, B. B., Aiello, I. W., and Fry, J. C., 2005, Deep sub-seafloor prokaryotes stimulated at interfaces over geological time: Nature, v. 436, p. 390–394, http://dx.doi.org/10.1038/nature03796

Phelps, T. J., Murphy, E. M., Pfiffner, S. M., and White, D. C., 1994, Comparison between geochemical and biological estimates of subsurface microbial activities: Microbial Ecology, v. 28, n. 3, p. 335–349, http://dx.doi.org/10.1007/BF00662027

Pirt, S. J., 1965, The maintenance energy of bacteria in growing cultures: Proceedings of the Royal Society London B, v. 163, n. 991, p. 224–231, http://dx.doi.org/10.1098/rspb.1965.0069

——— 1987, The energetics of microbes at slow growth rates: Maintenance energies and dormant organisms: Journal of Fermentation Technology, v. 65, n. 2, p. 173–177.

Price, P. B., and Sowers, T., 2004, Temperature dependence of metabolic rates for microbial growth, maintenance, and survival: Proceedings of the National Academy of Sciences of the United States of America, v. 101, n. 13, p. 4631–4636, http://dx.doi.org/10.1073/pnas.0400522101

Rinker, K. D., and Kelly, R. M., 2000, Effect of carbon and nitrogen sources on growth dynamics and exopolysaccharide production for the hyperthermophilic archaeon *Thermococcus litoralis* and bacterium *Thermotoga maritima*: Biotechnology and Bioengineering, v. 69, n. 5, p. 537–547, http://dx.doi.org/10.1002/1097-0290(20000905)69:5<537::AID-BIT8>3.0.CO;2-7

Rittman, B. E., and McCarty, P. L., 2001, Environmental Biotechnology: Principles and Applications: New York, McGraw-Hill, 768 p.

Robinson, J. A., and Tiedje, J. M., 1984, Competition between sulfate-reducing and methanogenic bacteria for H_2 under resting and growing conditions: Archives of Microbiology, v. 137, n. 1, p. 26–32, http://dx.doi.org/10.1007/BF00425803

Roszak, D. B., and Colwell, R. R., 1987, Survival strategies of bacteria in the natural environment: Microbiological Reviews, v. 51, n. 3, p. 365–379.

Røy, H., Kallmeyer, J., Adhikari, R. R., Pockalny, R., Jørgensen, B. B., and D'Hondt, S., 2012, Aerobic microbial respiration in 86-million-year-old deep-sea red clay: Science, v. 336, n. 6083, p. 922–925, http://dx.doi.org/10.1126/science.1219424

Russell, J. B., and Cook, G. M., 1995, Energetics of bacterial growth: Balance of anabolic and catabolic reactions: Microbiological Reviews, v. 59, n. 1, p. 48–62.

Schippers, A., Neretin, L. N., Kallmeyer, J., Ferdelman, T. G., Cragg, B. A., Parkes, R. J., and Jørgensen, B. B., 2005, Prokaryotic cells of the deep sub-seafloor biosphere identified as living bacteria: Nature, v. 433, p. 861–864, http://dx.doi.org/10.1038/nature03302

Scholten, J. C. M., and Conrad, R., 2000, Energetics of syntrophic propionate oxidation in defined batch and chemostat cocultures: Applied and Environmental Microbiology, v. 66, n. 7, p. 2934–2942, http://dx.doi.org/10.1128/AEM.66.7.2934-2942.2000

Schrum, H. N., Spivack, A. J., Kastner, M., and D'Hondt, S., 2009, Sulfate-reducing ammonium oxidation: A thermodynamically feasible metabolic pathway in subseafloor sediment: Geology, v. 37, n. 10, p. 939–942, http://dx.doi.org/10.1130/G30238A.1

Schulte, M. D., Shock, E. L., and Wood, R. H., 2001, The temperature dependence of the standard-state thermodynamic properties of aqueous nonelectrolytes: Geochimica et Cosmochimica Acta, v. 65, n. 21, p. 3919–3930, http://dx.doi.org/10.1016/S0016-7037(01)00717-7

Schulze, K. L., and Lipe, R. S., 1964, Relationship between substrate concentration, growth rate, and respiration rate of *Escherichia coli* in continuous culture: Archives of Microbiology, v. 48, n. 1, p. 1–20, http://dx.doi.org/10.1007/BF00406595

Segers, R., 1998, Methane production and methane consumption: a review of processes underlying wetland methane fluxes: Biogeochemistry, v. 41, n. 1, p. 23–51, http://dx.doi.org/10.1023/A:1005929032764

Shock, E. L., and Helgeson, H. C., 1988, Calculation of the thermodynamic and transport properties of aqueous species at high pressures and temperatures—Correlation algorithms for ionic species and equation of state predictions to 5 kb and 1000°C: Geochimica et Cosmochimica Acta, v. 52, n. 8, p. 2009–2036, http://dx.doi.org/10.1016/0016-7037(88)90181-0

——— 1990, Calculation of the thermodynamic and transport properties of aqueous species at high pressures

and temperatures - Standard partial molal properties of organic species: Geochimica et Cosmochimica Acta, v. 54, n. 4, p. 915–945, http://dx.doi.org/10.1016/0016-7037(90)90429-O

Shock, E. L., and Holland, M. E., 2004, Geochemical energy sources that support the subseafloor biosphere, *in* Wilcock, W. S. D., DeLong, E. F., Kelley, D. S., Baross, J. A., and Cary, S. C., editors, The subseafloor biosphere at mid-ocean ridges: American Geophysical Union, Geophysical Monograph 144, p. 153–165, http://dx.doi.org/10.1029/144GM10

——— 2007, Quantitative Habitability: Astrobiology, v. 7, n. 6, p. 839–851, http://dx.doi.org/10.1089/ast.2007.0137

Shock, E. L., Helgeson, H. C., and Sverjensky, D. A., 1989, Calculation of the thermodynamic and transport properties of aqueous species at high pressures and temperatures—Standard partial molal properties of inorganic neutral species: Geochimica et Cosmochimica Acta, v. 53, n. 9, p. 2157–2183, http://dx.doi.org/10.1016/0016-7037(89)90341-4

Shock, E. L., Oelkers, E. H., Johnson, J. W., Sverjensky, D. A., and Helgeson, H. C., 1992, Calculation of the thermodynamic properties of aqueous species at high pressures and temperatures—Effective electrostatic radii, dissociation constants and standard partial molal properties to 1000 °C and 5 kbar: Journal of the Chemical Society, Faraday Transactions, v. 88, n. 6, p. 803–826, http://dx.doi.org/10.1039/ft9928800803

Shock, E. L., McCollom, T. M., and Schulte, M. D., 1995, Geochemical constraints on chemolithoautotrophic reactions in hydrothermal systems: Origins of Life and Evolution of the Biosphere, v. 25, n. 1–3, p. 141–159, http://dx.doi.org/10.1007/BF01581579

Snow, C. L., Lilova, K. I., Radha, A. V., Shi, Q., Smith, S., Navrotsky, A., Boerio-Goates, J., and Woodfield, B. F., 2013, Heat capacity and thermodynamics of a synthetic two-line ferrihydrite, $FeOOH\text{-}0.027H_2O$: The Journal of Chemical Thermodynamics, v. 58, p. 307–314, http://dx.doi.org/10.1016/j.jct.2012.11.012

Steven, B., Léveillé, R., Pollard, W. H., and Whyte, L. G., 2006, Microbial ecology and biodiversity in permafrost: Extremophiles, v. 10, n. 4, p. 259–267, http://dx.doi.org/10.1007/s00792-006-0506-3

Stevens , T., 1997, Lithoautotrophy in the subsurface: FEMS Microbiology Reviews, v. 20, n. 3–4, p. 327–337, http://dx.doi.org/10.1111/j.1574-6976.1997.tb00318.x

Strapoć, D., Mastalerz, M., Dawson, K., Macalady, J., Callaghan, A. V., Wawrik, B., Turich, C., and Ashby, M., 2011, Biogeochemistry of micorbial coal-bed methane: Annual Review of Earth and Planetary Sciences, v. 39, p. 617–656, http://dx.doi.org/10.1146/annurev-earth-040610-133343

Strous, M., Kuenen, J. G., and Jetten, M. S. M., 1999, Key physiology of anaerobic ammonium oxidation: Applied and Environmental Microbiology, v. 65, p. 3248–3250.

Sverjensky, D. A., Shock, E. L., and Helgeson, H. C., 1997, Prediction of the thermodynamic properties of aqueous metal complexes to 1000 °C and 5 kb: Geochimica et Cosmochimica Acta, v. 61, n. 7, p. 1359–1412, http://dx.doi.org/10.1016/S0016-7037(97)00009-4

Tanger, J. C., IV, and Helgeson, H. C., 1988, Calculation of the thermodynamic and transport properties of aqueous species at high pressures and temperatures—Revised equations of state for the standard partial molal properties of ions and electrolytes: American Journal of Science, v. 288, n. 1, p. 19–98, http://dx.doi.org/10.2475/ajs.288.1.19

Teske, A. P., 2005, The deep subsurface biosphere is alive and well: TRENDS Microbiology, v. 13, n. 9, p. 402–404, http://dx.doi.org/10.1016/j.tim.2005.07.004

Teske, A., Callaghan, A. V., and LaRowe, D. E., 2014, Biosphere frontiers of subsurface life in the sedimented hydrothermal system of Guaymas Basin: Frontiers in Microbiology-Extreme Microbiology, v. 5, p. Article 362, http://dx.doi.org/10.3389/fmicb.2014.00362

Thorn, P. M., and Ventullo, R. M., 1988, Measurement of bacterial-growth rates in subsurface sediments using the incorporation of tritiated-thymidine into DNA: Microbial Ecology, v. 16, n. 1, p. 3–16, http://dx.doi.org/10.1007/BF02097401

Thullner, M., Dale, A. W., and Regnier, P., 2009, Global-scale quantification of mineralization pathways in marine sediments: A reaction-transport modeling approach: Geochemistry, Geophysics, Geosystems, v. 10, n. 10, p. 1–24, http://dx.doi.org/10.1029/2009GC002484

Tijhuis, L., van Loosdrechy, M. C. M., and Heijnen, J. J., 1993, A thermodynamically based correlation for maintenance Gibbs energy requirements in aerobic and anaerobic chemotrophic growth: Biotechnology and Bioengineering, v. 42, n. 4, p. 509–519, http://dx.doi.org/10.1002/bit.260420415

van Bodegom, P., 2007, Micorbial maintenance: A critical review of its quantification: Microbial Ecology, v. 5, n. 4, p. 513–523, http://dx.doi.org/10.1007/s00248-006-9049-5

Wang, G., Spivack, A. J., Rutherford, S., Manor, U., and D'Hondt, S., 2008, Quantification of co-occurring reaction rates in deep subseafloor sediments: Geochimica et Cosmochimica Acta, v. 72, n. 14, p. 3479–3488, http://dx.doi.org/10.1016/j.gca.2008.04.024

Wang, G., Spivack, A. J., and D'Hondt, S., 2010, Gibbs energies of reaction and microbial mutualism in anaerobic deep subseafloor sediments of ODP Site 1226: Geochimica et Cosmochimica Acta, v. 74, n. 14, p. 3938–3947, http://dx.doi.org/10.1016/j.gca.2010.03.034

Wankel, S. D., Joye, S. B., Samarkin, V. A., Shah, S. R., Friederich, G., Melas-Kyriazi, J., and Girguis, P. R., 2010, New constraints on methane fluxes and rates of anaerobic methane oxidation on a Gulf of Mexico brine pool via *in situ* mass spectrometry: Deep-Sea Research Part II-Topical Studies in Oceanography, v. 57, n. 21–23, p. 2022–2029, http://dx.doi.org/10.1016/j.dsr2.2010.05.009

Wankel, S. D., Germanovich, L. N., Lilley, M. D., Genc, G., DiPerna, C. J., Bradley, A. S., Olson, E. J., and Girguis, P. R., 2011, Influence of subsurface biosphere on geochemical fluxes from diffuse hydrothermal fluids: Nature Geoscience, v. 4, p. 461–468, http://dx.doi.org/10.1038/ngeo1183

Whitman, W. B., Coleman, D. C., and Wiebe, W. J., 1998, Prokaryotes: The unseen majority: Proceedings of the National Academy of Sciences of the United States of America, v. 95, n. 12, p. 6578–6583, http://dx.doi.org/10.1073/pnas.95.12.6578